

UNIVERSIDADE DE LISBOA
FACULDADE DE CIÊNCIAS
DEPARTAMENTO DE BIOLOGIA VEGETAL



**Is ARPC5 required for maintaining the equilibrium between Cancer Stem Cells
and non-Stem Cancer Cells?**

Maria Clara Barreto Carromeu Gomes

Mestrado em Biologia Molecular e Genética

Dissertação orientada por:

Florence Janody

Gabriela Rodrigues

2018

ABSTRACT

Nowadays, breast cancer is still a predominant cause of death in women despite all the available therapies. The malignancy, aggressiveness, and recurrence of breast cancer are believed to be caused by the presence of a specific tumorigenic cell subpopulation, termed Cancer Stem Cell (CSC) or tumor-initiating cell population. The cells of this cell population have been isolated from diverse breast tumors and from established breast cancer cell lines. They exist as a minority population within tumors and are defined by their ability to self-renew under non-differentiation conditions, to resist standard chemotherapeutic drugs and radiotherapy, to differentiate into non-stem cancer cells (NSCCs) and to recapitulate the tumor of origin both morphologically and phenotypically upon injection in immune-deficient mice. Conversely, NSCCs can convert into CSCs under certain conditions, indicating that CSCs and NSCCs do not exist in static states but instead are highly plastic, being able to interconvert between states. However, the origin of cells with stemness properties, as well as their relationships to NSCCs, is poorly understood.

CSCs and NSCCs exhibit distinct cell shape, mechanic, adhesion and mobility properties. All these processes are underlined by the actin cytoskeleton, which organizes into distinct actin filaments (F-actin) subtypes to perform these different functions. Consistent with a role for the actin cytoskeleton in promoting CSCs properties, reducing actin-myosin contractility strongly confers cancer stemness features. F-actin assembly, disassembly, and organization into distinct subtypes are controlled by a plethora of actin-binding proteins (ABPs). Among these ABPs, ARPC5 and ARPC5L, both encode for the ARPC5 subunit of the Arp2/3 complex. This complex is composed of seven subunits, which catalyzes the polymerization of new "daughter" actin filaments from the side of an existing filament, forming branched actin networks. Strikingly, ARPC5 and ARPC5L appear to have antagonistic effects on F-actin assembly.

Using the MCF10A cell line with conditional activation of the Src oncoprotein (MCF10A-ER-Src), which recapitulates the multistep development of breast cancer, the Actin Dynamic's lab observed that ARPC5L re-localizes to F-actin-rich structures that bridge cells between each other. The assembly of these bridges is concomitant with the differentiation of a pool of CSCs. In this work, I analyzed the composition and dynamical assembly of F-actin bridges during the transformation of the MCF10A-ER-Src cells and tested the hypothesis that the F-actin bridges, assembled by ARPC5 affect the acquisition of CSC properties.

My results show that F-actin bridges assemble between 12 and 24 hours after Src induction and contain both ARPC5 isoforms – ARPC5 and ARPC5L. Furthermore, my results show that F-actin bridges also contain tropomyosin 1.6/1.7, which could indicate a role for F-actin bridges in regulating CSCs since Tpm 1.7 recruits fascin that is critical for CSC pool maintenance. Lastly, knocking down ARPC5 appears to decrease the mammosphere forming efficiency of cells with conditional Src activation, suggesting that ARPC5 could promote the acquisition of CSC properties. Altogether, my data suggest that ARPC5 has an important function in tumorigenesis, although further studies are needed.

Keywords: Breast cancer; actin filaments; Cancer Stem Cells; Cellular transformation; ARPC5; ARPC5L.

RESUMO

Até aos dias de hoje, o cancro da mama continua a ser um dos mais predominantes e mortíferos cancros nas mulheres. A medicina e investigação científica têm, nos últimos anos, surtido resultados encorajadores no desenvolvimento de novas terapias para o combater. No entanto, tratamentos como a cirurgia, radioterapia, quimioterapia, imunoterapia, terapia hormonal e transplantes de células estaminais aumentam as chances de sobrevivência mas não a asseguram. A malignidade e agressividade do cancro da mama é, em grande parte, causada pela presença de células tumorais particulares com propriedades de auto-renovação, resistentes às terapias convencionais, denominadas de células estaminais cancerígenas ou formadoras de tumor. Estas células já foram isoladas de vários cancros da mama e de linhas celulares mamárias. Foram também associadas a processos tumorais de diferenciação de células cancerígenas não estaminais, de iniciação de tumores (morfologicamente e fenotípicamente) com a injeção em ratos imuno-deficientes. Para além disso, células cancerígenas não estaminais conseguem converter-se em células cancerígenas estaminais sob circunstâncias específicas, demonstrando que os estádios de ambas as subpopulações não são fixos e, assim, a plasticidade subjacente ao processo. No entanto, as origens destas subpopulações e as relações entre si ainda não foram clarificadas.

Células cancerígenas estaminais e não estaminais possuem características celulares distintas, no que diz respeito às suas propriedades na forma celular, mecânica, adesão e mobilidade. Todos estes processos são intimamente regulados pelo citoesqueleto de actina, que é composto por vários subtipos de filamentos de actina para desempenhar funções específicas. Consistente com o papel desempenhado pelo citoesqueleto de actina na promoção de propriedades estaminais nas células cancerígenas, foi observado que ao reduzir a contractilidade conferida pelo conjunto formado por actina e pela proteína miosina a estaminidade de células cancerígenas foi aumentada. A montagem dos filamentos de actina, desmontagem e organização em vários subtipos é controlada por várias proteínas que se ligam à actina. Entre elas, ARPC5 e ARPC5L são ambas codificantes para a subunidade ARPC5 do complexo Arp2/3. Este complex, composto por sete subunidades, cataliza a polimerização de novos filamentos de actina, ligando-se lateralmente a filamentos pre-existentes, formando assim redes de actina.

Com o objectivo de melhor compreender as primeiras fases do cancro da mama, foram feitos estudos com a transformação celular induzida pela administração de tamoxifen na linha epitelial MCF10A-ER-Src de células mamárias. Esta linha celular possibilita este estudo porque o composto tamoxifen ao se ligar aos receptores de estrogénio fundidos ao oncogene Src viral, induz uma alteração conformacional deste complexo, activando assim o oncogene e despoletando a transformação celular. Observou-se uma ocorrência simultânea de células com propriedades semelhantes às células estaminais cancerígenas, capazes de crescer em suspensão, com o mesmo perfil de expressão de marcadores – CD44^{alto}/CD24^{baixo} – e de células com a proteína ARPC5L localizada em estruturas ricas em F-actina (actina filamentosa) que ocorrem entre células. Estas observações permitem levantar a hipótese de que estas estruturas de F-actina podem estar associadas com a regulação da população de células estaminais cancerígenas. Através de estudos em células HeLa infectadas com o vírus *Vaccinia*, que necessita de construir uma cauda de F-actina para completar o seu ciclo de infecção, foi demonstrado que estas isoformas têm efeitos diferentes na actividade do complexo Arp2/3. A eficiência na polimerização de actina do complexo Arp2/3 é afectada dependendo da isoforma que o constitui, sendo que na ausência de ARPC5L os efeitos relativos ao comprimento da cauda e à velocidade em que a mesma foi construída foram opostos aos encontrados na ausência de ARPC5. Assim, sem ARPC5 as caudas encontradas são mais compridas, e o vírus tem uma movimentação mais rápida na célula, em comparação com as observações sem ARPC5L. Para além disso, estudos também demonstraram que ARPC5L promove a formação de estruturas de actina nas células associadas à invasão dos tecidos, denominadas de invadopodia, ao contrário de ARPC5. Assim, com estas observações relativas às actividades de ARPC5 e ARPC5L, pode-se inferir que estas proteínas têm especificidade de função.

Neste estudo eu analisei a composição e dinâmica destas pontes de actina que ocorrem entre células durante a transformação da linha celular MCF10A-ER-Src e testei a hipótese de que estas pontes, construídas pela proteína ARPC5, afectam a aquisição de propriedades estaminais em células cancerígenas. Assim, através de ensaios de imunofluorescência, observei que a formação destas estruturas ocorre entre as 12h e as 24h após a transformação ser induzida. Para além disso, observei a presença simultânea de ARPC5 com a presença de ARPC5L nas referidas estruturas de F-actina entre as células interconectadas pelas pontes de actina, o que demonstra que ambas podem coexistir nas pontes de F-actina. Na tentativa de obter informação funcional sobre as pontes de actina, proteínas associadas a funções particulares na célula e a comportamentos observados nas células cancerígenas foram analisadas com ensaios de imunofluorescência. Foi observada a presença da tropomiosina 1.6/1.7 nas pontes de actina, o que sugere um papel na regulação das células cancerígenas estaminais para as pontes de actina, uma vez que a tropomiosina 1.7 recruta a proteína fascina que está envolvida na manutenção da proporção das células cancerígenas estaminais. Observei também as propriedades estaminais nas células transformadas através de estudos com mamíferas, que avaliam a capacidade das células crescerem em suspensão e de proliferarem a partir de uma só célula, em conjunto com o “knockdown” direccionado a ARPC5. Foi observado um decréscimo de células com as características de células cancerígenas estaminais na ausência de ARPC5 e em condições de transformação celular induzida com tamoxifen. Estas observações sugerem que ARPC5 possa estar relacionado com a aquisição de propriedades estaminais por células cancerígenas. Quando considerados em conjunto, estes resultados sugerem uma associação entre a aquisição de propriedades de células estaminais cancerígenas e a construção das pontes de actina em células transformadas e a expressão de ARPC5, apesar de mais estudos serem necessários para compreender o processo.

Estruturas de F-actina, similares às observadas, já foram descritas em processos imunológicos que têm como principal função a transmissão de um sinal entre células através da construção de uma plataforma de sinalização, denominada de sinapse imunológica. Esta estrutura possui receptores de membrana e estruturas de actina, que juntamente com moléculas de adesão, como integrinas e caderinas, possibilitam a aproximação das células e a asseguram a estabilidade da estrutura durante a transmissão de sinal. Assim, neste contexto, uma estrutura semelhante poderia ocorrer nas células MCF10A-ER-Src transformadas com tamoxifen para permitir a ligação de determinados receptores da célula que envia o sinal a ligandos dispostos na membrana da célula que o recebe. As pontes de actina poderiam assim assistir na aproximação das células durante a transmissão de sinal, juntamente com moléculas de adesão. As pontes de actina observadas neste estudo podem, assim, corresponder a vestígios da intercomunicação celular ocorrida. Uma vez que os receptores da família Notch estão implicados na diferenciação de células do cancro da mama, assim como na sua renovação, é então levantada a hipótese de que receptores Notch podem estar envolvidos na transmissão de sinal que ocorreria nestas plataformas de sinalização. Tratam-se de receptores de membrana que ao se ligarem aos ligandos transmembranares da célula adjacente, desencadeiam uma alteração proteica nesses mesmos ligandos, que por sua vez vão migrar para o núcleo e através de uma cascata de sinalização, induzir a alteração do perfil de expressão dessa mesma célula, fazendo com que genes relacionados com a aquisição de propriedades de células estaminais cancerígenas sejam expressos. Estudos de quantificação proteica de ARPC5 foram também efectuados durante as etapas de transformação celular estudadas, que mostraram valores estáveis de expressão para ARPC5 com a crescente activação do oncogene Src, o que indica que, apesar de ocorrerem mais células interconectadas por pontes de actina a partir das 24 horas, os valores proteicos de ARPC5 não se alteram. Por outro lado, a quantificação proteica já adquirida para ARPC5L mostrou um aumento dos valores proteicos de ARPC5L após o aumento de formação das pontes de actina e posterior estabilização. Estas observações sugerem uma inibição da formação das pontes de actina por ARPC5L que pode levar à despolimerização das mesmas, e que está em conformidade com a especificidade de função celular que o complexo Arp2/3 tem dependendo das subunidades que o constituem. Uma vez que filamentos de actina produzidos por ARPC5L são menos estáveis e mais vulneráveis à despolimerização, quando moléculas estabilizadoras como a cortactina estão ausentes, a célula poderia regular a expressão destas proteínas para controlar a despolimerização das pontes de actina, o que não afectaria os filamentos

produzidos por ARPC5 pois as moléculas estabilizadoras não se ligam aos mesmos. Assim, e apesar de ambas as isoformas formarem complexos funcionais na polimerização de actina, a competitividade entre elas pelas restantes subunidades do complexo pode levar à sobreposição da actividade de uma isoforma sobre a outra e assim levar à despolimerização das pontes de actina quando a actividade de ARPC5L se sobrepõe à actividade de ARPC5.

Palavras-chave: Cancro da mama; F-actina; Células cancerígenas estaminais; Transformação celular; ARPC5; ARPC5L

TABLE OF CONTENTS

INTRODUCTION.....	6
1. Tumor heterogeneity in breast cancer progression.	6
2. Actin regulation: a central contributor of the CSC and NSCC states and plasticity	7
3. F actin-based structures	8
4. ABPs and cancer progression.....	8
4.1. Actin Isoforms.....	8
4.2. Tropomyosin Isoforms	9
4.3. Arp2/3 complex variations	9
5. Hypothesis and Aims	11
MATERIALS & METHODS	12
1. Cell lines, culture conditions and drug treatments.	12
2. Immunofluorescence analysis.	12
3. Immunoblotting analysis and quantification.	13
4. siRNA transient transfection.....	13
5. Mammosphere assay.....	13
RESULTS	14
1. TAM-treated ER-Src cells assemble transient F-actin bridges 24 hours after TAM treatment.	14
2. Tpm1.6/1.7, as well as γ - and β -actin, localizes to F-actin bridges in ER-Src treated cells with TAM for 24 hours.....	15
3. ARPC5 localizes with ARPC5L at F-actin bridges in ER-Src cells, 24 hours after TAM treatment.	18
4. Unlike ARPC5L, ARPC5 levels are not altered in ER-Src cells during the 36 hours of TAM treatment.	18
5. ARPC5 could be required to assemble the F-actin bridges 24 hours after TAM treatment.	20
6. ARPC5 does not alter the frequency of epithelial and mesenchymal cell populations in ER-Src cells treated with TAM for 24 hours.....	21
7. ARPC5 could increase the mammosphere-forming abilities of TAM-treated ER-Src cells.	24
DISCUSSION	25
1. F-actin bridges resemble Immunological Synapses and could act as “signaling platforms”.	25
2. ARPC5 and ARPC5L could play opposite functions on F-actin bridge assembly.....	26
3. ARPC5 could promote Cancer Stem Cell features through F-actin bridge assembly.	26
4. Model: ARPC5-containing F-actin bridges could assist in intercellular communication to trigger the CSC program.	27
ANNEXES.....	28
REFERENCES.....	29

INTRODUCTION

1. Tumor heterogeneity in breast cancer progression.

The leading form of cancer in women worldwide is breast cancer accounting for 2.1 million occurrences each year and being responsible for approximately 15% of all cancer deaths among women, according to World Health Organization data from 2018¹.

It is believed that breast cancer initiates in either the epithelium of the lobules, which are the milk-producing glands, or the ducts, which connect the glands to the nipple, upon genetic and epigenetic changes in oncogenes and tumor suppressor genes. Breast cancer develops in a multi-stage manner, through which mammary cells acquire uncontrolled growth, proliferative and survival advantages. Progressively, in some of the cases, premalignant cells acquire migratory and invasive properties, taking advantage of the body's circulatory system to metastasize in secondary sites².

One major cause of breast cancer therapy failure is due to the cellular inter- and intra-tumor heterogeneity, characterized by different cell populations with distinct phenotypes, and various levels of aggressiveness. To explain intra-tumor heterogeneity researchers have suggested two models. The clonal evolution model, or stochastic model, states that tumor development is driven by the accumulation of spontaneous epigenetic modifications and genetic mutations through repeated cell divisions as well as by interactions with the microenvironment, which culminates in the selection of the most competitive clones and promotes tumor formation. According to this model, any premalignant cell from a tumor that has not acquired invasive and metastatic properties can become a cancer cell, as long as it has a selective advantage over its neighbor cells in the primary tumor site. The cancer stem cell model, or hierarchy model, states that tumor development is established by restricted pools of cells with self-renewing properties, known as Cancer Stem Cells (CSCs) or Tumor-initiating Cells (TICs). Based on this theory, tumors would be hierarchically organized with a few undifferentiated

CSC at the top of the hierarchy and differentiated Non-Stem Cancer Cells (NSCCs) forming the tumor. CSCs can initiate and maintain tumors, as well as spread cancer to secondary sites³. In 1997, researchers demonstrated the

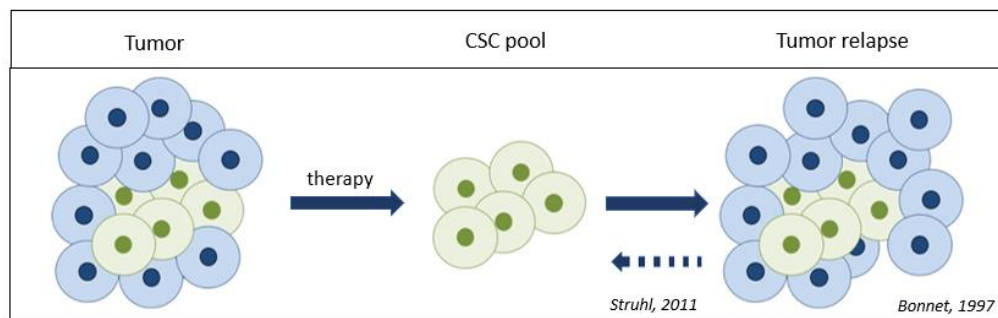


Figure 1: Cancer Stem Cell population in the tumor as a cell population able to resist to conventional therapies, unlike Non-Stem Cancer Cells, and restarting a new tumor. Also, in certain conditions, NSCCs were showed to also give rise to CSCs.

(inspired from: <https://hsci.harvard.edu/stem-cells-and-cancer>)

existence of CSCs by showing that primary leukemia cancer cells injected into immune-deficient mice were able to differentiate, proliferate and develop into leukemia⁴. While conventional therapy can kill the bulk of cancer cells⁵, CSCs are resistant to it⁶, playing a major role in tumor relapse, as it is shown in Figure 1.

Moreover, there is growing evidence for a tight plasticity associated to this process and that tumors are hierarchically organized but dynamically maintained with CSCs that differentiate into NSCCs but also with NSCCs that recover stemness and “dedifferentiate” into CSCs. The bidirectional interconversion between these cell populations establishes that selective pressure and microenvironmental interactions regulate cell fate, changing tumorigenic potential. Importantly, bidirectional interconversion has been observed *in vitro*, in the human mammary epithelial cell line MCF10A with conditional Src activation and in cells from breast tumors. By studying these cases, researchers reported the maintenance of the proportion of both cell

populations over many generations and an IL-6 mediated conversion of NSCCs into CSCs. This dynamic equilibrium was being regulated by an intricate inflammatory signaling pathway to control the rate of CSC formation, which depended on the proportion of CSC in the population, the amount of IL-6 secreted by them, the response of NSCCs to IL-6 concentration and the concentration of IL-6 receptor⁷.

In the CSC field, it is believed that CSCs express a high level of CD44 (CD44^{high}) and low levels of CD24 (CD24^{low}), as this cell population displays CSC properties⁸. However, some researchers demonstrated that cells with the phenotype CD44^{high}/CD24^{high} have stem-like properties as well and that they can originate cells with the CSC phenotype⁹⁻¹¹. In addition, some basal-like breast cancers upregulate the cell-adhesion molecule P-cadherin, which has been proved to mediate stem cell properties in breast cancer, since it is associated with the increased capacity to grow spheres, to resist cell death and to express breast CSC markers, such as CD44, CD49f and aldehyde dehydrogenase. Furthermore, P-cadherin had higher levels in the CD44^{high}/CD24^{high} cell population, than in the CD44^{high}/CD24^{low} and the association with either CD44 or CD24, resulted in the worst patient prognosis when compared to other markers¹². In addition, functional studies demonstrated that P-cadherin oncogenic activity, associated with poor breast cancer prognosis¹³ and tumorigenesis¹⁴, is enhanced by E-cadherin expression at the cell membrane, since their coexpression further inhibited the formation of a strong adhesion complex by disrupting the interaction with E-cadherins and another cell adhesion molecules - catenins¹⁵.

Stem cell homeostasis is normally regulated by many molecular signaling pathways which interplay with each other, including the Hedgehog, Wnt and Notch signaling pathways. Notch signaling pathway is a highly conserved pathway that allows cells to communicate with each other, inducing cell fate decision, proliferation and apoptosis and maintaining homeostasis in adults and during embryonic development. Activation of Notch signaling requires the binding between a Notch ligand expressed on the surface of one cell and a Notch receptor expressed on the surface of another cell. For this interaction to take place, it is required that the cell sending the signal is close to the cell receiving it. Upon ligand-binding Notch receptors undergo proteolytic cleavage and the consequent release of an intracellular domain that is translocated to the nucleus and acts as a transcription regulator. In the context of breast cancer, the Notch signaling pathway has been shown to trigger differentiation and self-renewal of cancer cells, promoting therein tumorigenesis and the acquisition of CSC properties^{16,17}. However, what triggers the “CSC program” remains to be understood.

2. Actin regulation: a central contributor of the CSC and NSCC states and plasticity

CSCs and NSCCs exhibit very distinct cellular states and shape, mechanical, adhesion and mobility properties¹⁶⁻¹⁸. All these processes are underlined by the actin cytoskeleton, which organizes into distinct actin filament (F-actin) subtypes to perform these different functions. F-actin is subjected to dynamical non-stop cycles of assembly and disassembly, with new actin monomers (G-actin) being added at the 'barbed' end and being removed from the 'pointed' end. As simple as it may seem, actin polymerization is tightly regulated by several actin-binding proteins (ABPs) that produce different outcomes on actin. For instance the ABD formin contributes to the actin filament elongation and cofilin to its disassembly¹⁹. Consistent with a role of actin regulation, as a central contributor of the CSC and non-CSCs states and of their plasticity, studies in different cancers demonstrated that reducing actin-myosin contractility, strongly promotes stem cell characteristics²⁰⁻²². Moreover, actin deregulation is a main transcriptional signature of human myeloma cell lines resistant to chemotherapeutic inhibitors against Histone deacetylase. Combinatory treatment with agents targeting the actin cytoskeleton can overcome this resistance²³. Among ABPs involved, the F-actin bundling protein F-actin is a likely candidate, as it is involved in breast cancer chemotherapeutic resistance²⁴. However, disrupting the cytoskeletal balance using cytoskeletal cancer drugs had also yielded unexpected effects on the aggressiveness of tumor cells²⁵, indicating that the actin cytoskeleton has both beneficial and detrimental effects.

3. F actin-based structures

Fundamentally, actin fibers organize into bundles and networks to build actin structures associated with diverse cellular organelles and roles in the cell. To drive cell migration, motile cells produce a three-dimensional sheet-like membrane protrusion at the leading edge, called lamellipodium²⁶. Stress fibers, on the other hand, are structures composed of cross-linked actin filament bundles that function to maintain cellular tension, reshape the cytoskeleton and to signal in mechanotransduction. Also, stress fibers can be composed of myosin motor proteins, which give contractile properties to non-muscle cells, providing force for cell adhesion, migration and morphogenesis²⁷⁻²⁹. To sense the environment, cells have filopodia, which are slender cytoplasmic projections that extend beyond the leading edge, important in directed cell migration and cell-cell interactions³⁰. Podosomes, on the other hand, are conical adhesive structures placed on the outer surface of the plasma membrane that serve as sites of attachment and degradation of the extracellular matrix in cell migration. In cancer cells with high metastatic potential, structures similar to podosomes, called invadopodia, are capable of crossing extracellular barriers and of degrading the extracellular matrix more efficiently³¹.

F-actin is also involved in midbody formation: a transient cell-cell connection achieved through mitosis in somatic cells at the end of cytokinesis. These midbodies mark the site in which cells are abscised to form individual daughter cells and allow molecular passage between them²¹. Interestingly, midbodies in germ cell cytokinesis become stable and form a syncytium – multinucleated cell – with a permanent intercellular bridge (ICB), connecting cells through a cytoplasmic channel²². Moreover, during T-cell activation, F-actin cooperates in the assembly of a structure called immunological synapse (IS). This occurs as a migrating mature T cell encounters and engages with an antigen-presenting-cell through its T-Cell Receptors and adhesion molecules of low-affinity interaction. Consequentially, the resulting cluster rearranges, and the receptors become surrounded by adhesion molecules³². Furthermore, F-actin is also involved in the formation of membrane extensions named tunneling nanotubes (TNT), that originate from a thin cytoplasmic projection – the filopodium – and extend beyond the leading edge until they reach a neighboring cell and convert into a “bridge”. Alternatively, they can be formed by a thin membrane thread retained upon membrane dislodgement³³. Interestingly, a similar structure, named cytoneme, is found in *Drosophila melanogaster* that extends between morphogen-producing and target cells. They function as “highways” to transport organelles, vesicles and ions between distant cells and are found in immune cells²³ and in cancer cells contributing to tumorigenesis²⁴. Altogether, F-actin is proved to be involved in several functions essential for normal cell behavior, but F-actin can also promote tumorigenesis, demonstrated by its role in invadopodia assembly.

4. ABPs and cancer progression

4.1. Actin Isoforms

Mammals express six distinct actin isoforms, transcribed from six independent genes: two striated muscle (α -skeletal and α -cardiac), two smooth muscle (α - and γ -SMA) and two cytoplasmic (β - and γ -CYA). Muscle-associated actin isoforms are expressed in a tissue-specific manner, while cytoplasmic actin isoforms are ubiquitously expressed in all cells. Nevertheless, cytoplasmic actin isoforms display distinct subcellular localization and function, which changes depending on cell behavior. In spreading and stationary cells, β -CYA is preferentially localized at basal stress fibers, at filopodia, at cell-cell contacts and at circular bundles of fibroblastic and epithelial cells. γ -CYA was found at lamellar and dorsal cell regions. On the other hand, in moving cells, both isoforms were found at lamellipodia, but only β -CYA was found at stress fibers and focal adhesions and only γ -CYA in cell protrusions and at the dorsal cortex²⁵. Functional knockout studies in mouse fibroblasts showed that β -CYA promotes cell growth, migration and regulates G-actin availability³⁴, which points to a role in promoting tumorigenesis. In contrast, γ -CYA could have a tumor suppressor effect

since its depletion in neuroblastoma cells reduced mitotic arrest and enhanced centrosome amplification of cancer cells³⁵.

4.2. Tropomyosin Isoforms

Tropomyosins are expressed from four different genes that originate over forty isoforms by alternative splicing. They are classified as low molecular weight (LMW), if they have between 28 to 33 kDa, and high molecular weight (HMW), if they have between 34 to 40 kDa. Tropomyosins function as F-actin stabilizers by binding to actin subunits along the actin filament and mediate the access of various ABPs to F-actin. Each of these isoforms associates with distinct F-actin structures to control specific cellular functions³⁶.

In cancer, some tropomyosin isoforms appear to display a tumor suppressor effect³⁷, while others have the opposite effect³⁸. The HMW tropomyosin 1.6 (or Tm2) was found to rescue cells from their transformed state, by promoting cell spreading and focal adhesion contacts³⁹, and to stabilize stress fiber, as its depletion increased actin filament dynamics and led to a complete loss of these structures⁴⁰. HMW tropomyosin 1.7 (or Tm3) is also associated with stable actin filaments⁴⁰ but preferentially binds to fascin⁴¹, which promotes metastasis⁴², inhibits tumor suppressor activity and maintains the CSC pool in breast cancer⁴³. The LMW tropomyosins 1.8 (or Tm5a) and 1.9 (or Tm5b) localize at cell-to-cell contacts of epithelial cells⁴⁴ and were demonstrated to regulate mammary gland differentiation. Both were suggested to cooperate with cell-cell adhesion molecules to stabilize and maintain the integrity of epithelial cell junctions⁴⁵. The LMW tropomyosin 3.1 (or Tm5NM1) is essential for ERK-mediated proliferation, as phosphorylated ERK fails to translocate to the nucleus in the absence of tropomyosin 3.1⁴⁶. Tropomyosin 3.1 also stabilizes focal adhesions and prevents cell migration during wound healing, which suggests a regulatory role in cell motility and migration^{47,48}. In contrast, LMW tropomyosin 4.2 (or Tm4) gives stress fibers their contractile behavior by interacting with myosin II⁴⁰, which is required to increase the proto-oncogene tyrosine-protein kinase Src activation and cancer progression⁴⁹.

4.3. Arp2/3 complex variations

Actin can be polymerized on the side of a pre-existing filament to produce branches and consequently dense actin networks, that exert a pushing force in the cell, required to form, maintain and reshape the cytoskeleton and cell membrane. This branched nucleation is performed by the Arp2/3 protein complex, depicted in Figure 2, which is composed of seven proteins in its canonical form: Arp2, Arp3 and ARPC1 through ARPC5. Arp2/3 complex exists in an inactive conformation, but upon interaction with WASP and WAVE family proteins becomes activated and by mimicking an actin monomer, Arp2/3 binds to the mother filament, mostly achieved through the backbone formed by ARPC2 and ARPC4 subunits¹⁸, and polymerizes actin at an angle of approximately 70° from the original filament. The Arp2/3 complex-dependent nucleation has been shown to have a determinant role in lamellipodium assembly and cell migration⁵⁰.

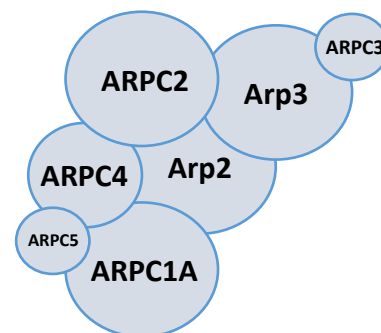


Figure 2: Arp2/3 complex and its subunits Arp2, Arp3, ARPC1, ARPC2, ARPC3, ARPC4 and ARPC5.

(inspired from Fig. 1 of reference 60)

In cancer, some Arp2/3 subunits were found to be overexpressed, which could be an indicator of an enhanced Arp2/3 complex activity. Arp2 subunit was reported to be overexpressed in isolated cells from different cancer types, concomitantly with an overexpression of the Arp2/3 activator WAVE2^{51,52}, further suggesting a strong association between Arp2/3 activity and cancer progression. Adding to that, ARPC2 and ARPC5 were reported to be overexpressed in invasive carcinoma cells extracted from breast cancer cell lines⁵³ and ARPC5 was also overexpressed in mice mammary tumors together with ARPC3⁵⁴. Moreover, in colorectal cancer, the Arp2 subunit is overexpressed⁵⁵. Also, Arp2/3 dysregulation can lead to invasion and metastasis²⁰, when Arp2/3 complex further reshapes the cytoskeleton and cell membrane to produce

invadopodia⁵⁶. Cancer cells take advantage of this actin structure to degrade and cross the extracellular matrix by thriving their way to blood vessels and promote metastasis^{57,58}, but also to co-opt preexisting blood vessels and promote tumor growth⁵⁹. Further studies show an association between Arp2/3 overexpression and poor patient survival in lung⁵² and breast cancer⁵¹.

Recent studies have demonstrated that the Arp2/3 complex exists in alternative forms, depending on the composition of the complex and each of these complexes appear to have different effects on actin filaments⁶⁰. Thus, the ARPC5 subunits – ARPC5 and ARPC5L – are encoded by two genes 67% identical. Using infected HeLa cells with vaccinia virus, which exploits the cell's Arp2/3 complex-mediated actin assembly to build a tail to move in the cytoplasm, the Way's laboratory has shown that in the absence of ARPC5, virus forms a longer actin tail and moves faster, while, in the absence of ARPC5L, the actin tail is shorter, which results in slower motility⁶¹. In addition, ARPC5 isoforms have distinct effects on invadopodia assembly. While knocking down ARPC5 increases invadopodia formation, reducing ARPC5L function has the opposite effect (M. Way, personal communication), suggesting a role of ARPC5L in tumor cell invasion. However, ARPC5 was also shown to contribute to cell migration and invasion in head and neck squamous cell cancer tissues, in which their expression levels are increased and decreased with the activity of miR-133 tumor suppressor^{62,63}.

In the Actin Dynamics Lab, ARPC5L was found to be upregulated in pre-invasive breast tumor samples and during the transformation of the breast epithelial cell line MCF10A-ER-Src (ER-Src)⁴⁹. The MCF10A-ER-Src cell line contains a fusion between the oncogenic viral non-receptor tyrosine kinase (v-Src) and the ligand-binding domain of the Oestrogen Receptor (ER). Upon tamoxifen (TAM) administration, this molecule binds to ER, changing ER-Src complex conformation, and triggers Src proto-oncogene activation^{64,65}. Src functions in cell

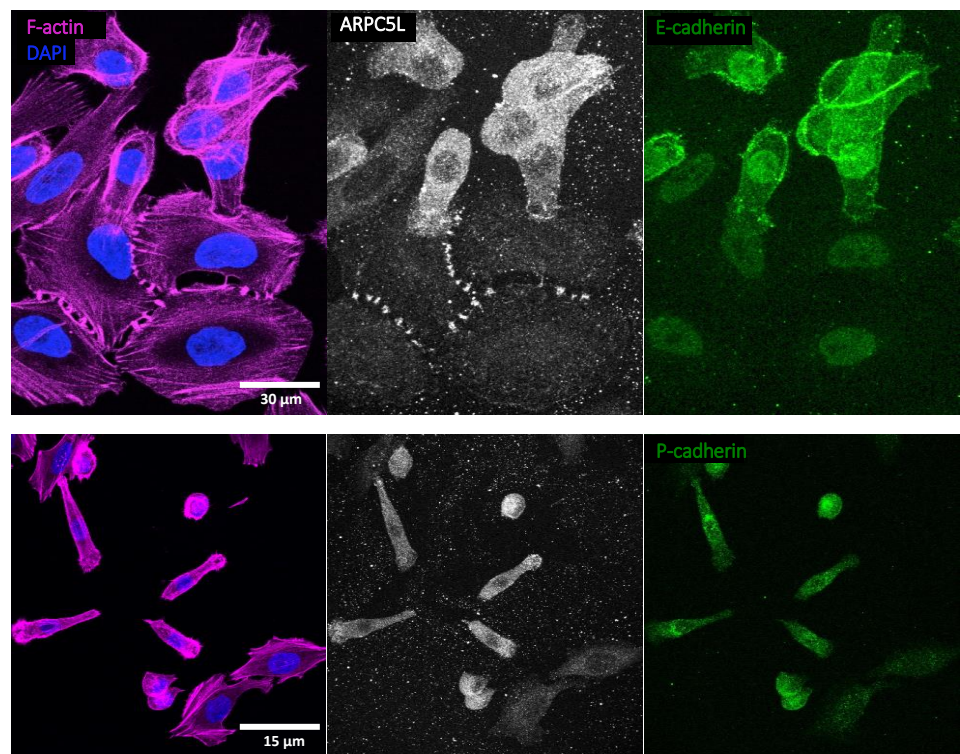


Figure 3: MCF10A-ER-Src cells after 24h of TAM treatment. Subpopulation of cells displaying F-actin bridges with ARPC5L and expressing low levels of both E- and P-cadherin. Mesenchymal cell subpopulation expresses high levels of both cadherins, which could indicate that these cells are CSCs.

(data from M. Araújo – Actin Dynamics lab)

signaling and assists in the control of cell adhesion, growth, movement and differentiation. In breast cancer, Src protein levels and activity are increased in malignant and non-malignant breast tumors and are associated with decreased survival^{66,67}. Src induction after 12h of TAM exposure was found to promote transient stress fiber assembly and cell signaling pathway upregulation that further enhanced Src activity and cell proliferation⁴⁹. However, the transformation process starts with Src triggering an inflammatory response by activating NF- κ B cytokine which leads to the IL-6 cytokine activation at 36h, culminating in a positive feedback loop since IL-6 also activates NF- κ B. Therefore, the resulting epigenetic switch from non-transformed to transformed cells⁶⁵, leads to a fully transformed state within 24-36h, allowing the study of the

multistep development of breast cancer in a short amount of time^{49,64}. Moreover, in two- and three-dimensional cultures, MCF10A-ER-Src cells under TAM treatment acquire a progressive morphological transformation, which culminates in cell detachment and extrusion⁴⁹. Interestingly, 24 hours after TAM treatment, two distinct cell populations, shown in Figure 3, arise. One population assembles F-actin-rich bridges connecting these cells to each other, where ARPC5L localizes. In addition, this cell population spreads highly on the substratum and appears to express lower levels of the cell adhesion molecules E-cadherin and P-cadherin, as opposed to those that had acquired a mesenchymal phenotype. High P-cadherin levels are known to mediate stem-cell properties and to be associated with breast CSC¹², which could indicate an emergence of CSC properties in these mesenchymal cells. Accordingly, the assembly of F-actin bridges between TAM-treated ER-Src cells undergoing transformation is concomitant with the differentiation of a pool of CSCs, expressing high levels of CD44 (CD44^{high}) and low levels of CD24 (CD24^{low}) and capable of forming mammospheres⁷.

5. Hypothesis and Aims

Observations from the Actin Dynamics Lab suggest that the assembly of ARPC5L-positive F-actin bridges between cells undergoing transformation could be involved in the emergence of a pool of cells with CSC properties. Because ARPC5L and ARPC5 have distinct effects on actin polymerization, invadopodia and vaccinia virus actin tail assembly⁶¹, they can have an opposite function in F-actin bridges assembly and in regulating CSCs. The aim of this project is to test the role of ARPC5 in the assembly of the F-actin bridges during the transformation of the TAM-treated ER-Src cells and in the emergence of a pool of CSCs, as well as to identify relevant ABPs that compose these F-actin bridges.

To test these hypotheses, I will use the TAM-inducible ER-Src cell line to investigate the dynamic F-actin bridge assembly during transformation, as well as determine the actin and tropomyosin isoform composition of these bridges. I will determine if ARPC5 protein levels are altered during cellular transformation and compare ARPC5 and ARPC5L physical distributions in the cell. I will also use short-hairpin RNA to target ARPC5 for degradation to analyze the role of ARPC5 in the assembly of F-actin bridges, on ARPC5L subcellular localization and on the acquisition of cells with CSC features.

MATERIALS & METHODS

1. Cell lines, culture conditions and drug treatments.

The MCF10A-ER-Src (ER-Src) cell line was kindly provided by K. Struhl. Cells were grown in a humidified incubator at 37 °C, under a 5% CO₂ atmosphere in DMEM/F12 growth medium (Invitrogen, 11039-047), supplemented with 5% horse serum (Invitrogen 16050-122), previously stripped of hormones through dextran-coated charcoal incubation (Sigma C6241), 20 ng per ml of EGF (Peprotech, AF-100-15), 10 mg per ml of insulin (Sigma, I9278), 0.5 mg per ml of hydrocortisone (Sigma, H-0888), 100 ng per ml of cholera toxin (Sigma, C-8052), and 10 μ L per mL of penicillin/streptomycin (Invitrogen, 15070-063). To treat cells with 4OH-TAM or EtOH, 50% confluent cells were plated and allowed to adhere for about 24 h before treatment with 1 mM 4OH-TAM (Sigma, H7904) or with the identical volume of Absolute EtOH for the indicated time periods. For the serum starve experiments, cells were cultured in plain DMEM/F12 during the whole course of the experiments, either containing EtOH alone or 4OH-TAM diluted in EtOH,

2. Immunofluorescence analysis.

MCF10A-ER-Src cells were plated in poly-L-lysine-coated coverslips (Sigma, P-8920) with 13 millimeters of diameter. To stain cells for the actin isoforms (β -CYA; γ -CYA), epithelial cell monolayers were fixed with pre-warmed 1% paraformaldehyde in DMEM for 30 minutes and washed with PBS twice. For tropomyosin staining (CG β 6; δ /9d; α /1b; γ /9d), cells were fixed for 10 minutes with a solution composed of 16% formaldehyde (Polysciences, 18814), PIPES 0.2 M pH 6.8 (Sigma, P6757), HEPES 0.2 M pH 7 (Promega, H5302), EGTA 0.5M pH 6.8 (Sigma, E3889-100G), MgSO₄ 1M (Merck, 105886) and washed twice with PBS. For all other fluorescence staining, cells were fixed in 4% paraformaldehyde in PBS at pH 7 for 10 minutes, quenched in 0.1 M Tris pH 7.4. Permeabilization for cells stained for the actin isoforms and specific tropomyosin isoforms - CG β 6; δ /9d - was made with quick rinses of crescent followed by decrescent sequential methanol dilutions in phosphate-buffered solution (PBS) at 20%, 50%, 80 and 95%. For all other fluorescence staining, cells were permeabilized with TBS-T (TBS - 0.1% Triton X-100) at room temperature. After cells being washed twice with PBS, the ones stained for actin isoforms were blocked with 5% BSA in PBS and for all other fluorescence staining, cells were blocked with a solution composed of 1mM MES, 15 mM NaCl, 0.5 mM EGTA, 0.5 M MgCl₂, 0.5 M glucose, 2% (v/v) FBS, 1% (m/v) BSA in PBS at pH 6.1. Primary antibodies were incubated overnight at 4 °C in blocking solution with a final volume of 30 μ L per coverslip. Coverslips were then washed four times with PBS and incubated with secondary antibodies and with Phalloidin-conjugated (Sigma, P-1951) at 0.3mM in blocking solution with a final volume of 30 μ L per coverslip for 1 h at room temperature. After three washes in PBS, cells were stained with 2 mg of DAPI per ml (Sigma, D9542) for 5 minutes in PBS, washed again with PBS and mounted on Vectashield (Vector Labs, H-1000) and microscope slide (VWR, ECN 631-1552). The following primary antibodies were used: anti- β -CYA (1:50; mAb 4C2, IgG1, a gift from C. Chaponnier), anti- γ -CYA (1:100; mAb 2A3, IgG2b, a gift from C. Chaponnier), anti-ARPC5L (1:500, Abcam, ab169763), anti-ARPC5 (1:100, Synaptic Systems, 305011), anti-E-cadherin (1:200, Invitrogen, 131700), anti-E-cadherin (1:200, Cell Signaling, 3195), anti-P-cadherin (1:50, BD Biosciences, 610228), anti- α /1b (1:200, a gift from P.Gunning⁶⁸), anti- γ /9d (1:1000, a gift from P.Gunning⁶⁹), anti-CG β 6 (1:500, a gift from P.Gunning⁷⁰) and anti- δ /9d (1:500, a gift from P.Gunning^{71,72}). The secondary antibodies used to detect anti- β -CYA and anti- γ -CYA were anti-mouse IgG1 FITC-conjugated (1:50; Invitrogen, A21240) and anti-mouse IgG2b alexa 647-conjugated (1:50; Invitrogen, A21141), respectively. The secondary antibodies used to detect all other primary antibodies were IgG FITC (1:200, Jackson Immunoresearch) or Cy5 (1:200, Jackson Immunoresearch) Alexa Fluor 647-conjugated (1:800, Jackson Immunoresearch). Fluorescence images were obtained on a Leica SP5 confocal coupled to a Leica DMI6000, using the 40x and 63x 1.4 HCX PL APO CS

Oil immersion objective. DAPI channel was used to count cells for the quantifications of F-actin bridges and cell populations. The ImageJ 1.51j program was used to check for protein subcellular localization. The statistical analysis was performed with GraphPad Prism 6, using the statistical test one-way ANOVA.

3. Immunoblotting analysis and quantification.

Cells from 6-well plates were harvested by dissociation with 250 μ L of TrypLE Express (ThermoFisher, 12604-021) at 37°C for 15 minutes, followed by scraping and centrifugation at 1000 rpm for 5 minutes; supernatant was removed. Cells were then lysed with 100 μ L of Abcam lysis buffer containing protease (Roche, cOmplete Tablets, 4693159001) and phosphatase (Roche, PhosSTOP Tablets, 4906837001) inhibitors, Tris 10 mM pH 7.4, NaCl 100 mM, EDTA 1 mM, EGTA 1 mM, Triton X-100 1%, glycerol 10%, SDS 0.1%, sodium deoxycholate 0.5% in H₂O for 15 minutes on ice, followed by centrifugation at 14000 rpm for 30 minutes at 4°C. The protein quantification was performed using Bradford Assay (BIO-RAD, 500-0006) and Laemmli buffer (1X) was added. Cell lysates were then boiled at 95°C for 5 minutes, centrifuged at 8000 rpm for 5 minutes, loaded onto a SDS-PAGE gel, constituted of 5% stacking and 12% resolving gels, and run at 50v until Prestained Protein Standards (BIO-RAD, L001649A) bands were separated and at 120v until the end. Then, they were transferred to a PVDF membrane (BIO-RAD, 162-0177) using a wet transfer system with chilled transfer buffer and in a box full of ice at 100v for 65 minutes. Membranes were blocked with 5% milk in TBS 0.1% Tween 20 for 1 hour and incubated overnight with the following: rabbit anti-activated Src (1:1,000; Invitrogen, 44-660G), rabbit anti-GAPDH (1:2,000; Santa Cruz, 2D4A7) and anti-ARPC5L (1:500, Abcam, ab169763). Detection was performed by using HRP-conjugated antisera (Jackson ImmunoResearch) and Enhanced Chemi-Luminescence (Thermo Scientific, 32106) detection (Thermo Scientific, 32106). Membranes were washed four times after both antibody incubations. Western blots were quantified using Image Studio Lite. Uncropped scans of the most relevant western blots can be found in Supplementary Materials.

4. siRNA transient transfection.

Cells plated in a 6-well plate, with approximately 30% confluency, were washed with 2 mL of PBS and added 1,5 mL of transfection media, absent in horse serum, insulin and penicillin/streptomycin. Complexes mix, composed of siARPC5 SMARTpool (Dharmacon, M-012080-00) at a final concentration of 24nM and 12 μ L/well of transfection reagent HiPerFect (QUIAGEN, 301705) was added, after waiting 10 minutes, drop-by-drop in a circular motion. After 12 hours, transfection medium was replaced by complete growth medium and after 48 hours of transfection cells were ready for experiments. A negative siRNA control, with no homology to any gene, was also used (QUIAGEN AllStars Negative Control siRNA, 1027310).

5. Mammosphere assay.

6-well plates were coated with 2 mL of 12g/L of Poly (2-hydroxyethyl methacrylate) (SIGMA, P3932-10G). After filtered with a 0.45 μ m filter (Life Sciences, 12829254), 2mL per well of mammosphere medium was added, constituted of 20 μ L per mL of B27 (gibco, 17504-044), 500ng per mL of Hydrocortisone, 40 μ L per mL of insulin and 10 μ L per mL of penicillin/streptomycin. After cell dissociation with TrypLE Express and harvesting, a single cell population was generated by passing the cell suspension 3 times through a 25G gauge needle (Terumo, 160825). 7500 cells were plated in each well and were allowed to grow for 5 days, without media changing) and were imaged on a Leica HCScreening, using the 10x objective.

RESULTS

1. TAM-treated ER-Src cells assemble transient F-actin bridges 24 hours after TAM treatment.

According to the hypothesis that intercellular F-actin bridges formed under transformation could be controlling the acquisition of CSC properties, I looked at F-actin bridge occurrence, identity and assembly during Src-dependent cellular transformation. As expected, ER-Src cells treated with TAM and stained for Phalloidin to mark F-actin and DAPI, which stains the nucleus, showed progressive morphological alterations, characterized by the appearance of mesenchymal-like cells (Fig. 1a, yellow arrow), as well as highly spread cells not connected to other cells, forming spikes (Fig. 1a, green arrow) 36 hours after treatment. In contrast, cells treated with EtOH (negative control) maintained an epithelial-like morphology during all treatment, characterized by confluent cells assembling into a monolayer sheet (Fig. 1a, upper panels). As previously observed, in Figure 3 from Introduction, 24 hours after TAM treatment, two morphologically distinct populations of ER-Src cells could be observed. Some single cells displayed a mesenchymal-like morphology (Fig. 1a, lower panel, yellow arrow), while others were highly spread on the substratum and were interconnected with each other by F-actin-rich structures (F-actin bridges) (Fig. 1a, lower panels, white arrows). EtOH-treated control ER-Src cells, however, never displayed a mesenchymal morphology or cells connected to each other through F-actin bridges. To quantify the dynamic assembly of F-actin bridges during Src-induced cellular transformation, I evaluated their occurrence overtime in TAM-treated ER-Src cells during 36 hours of transformation. After 4 or 12 hours of TAM treatment, only rare cells interconnected by F-actin bridges could be observed. However, at 24 hours after TAM treatment, the number of interconnected cells significantly increased to reach 15,72 % on average. Interestingly, at 36 hours the number of interconnected cells slightly decreased to 10,15 %, although, not significantly when compared to the number of interconnected cells observed at 24 hours (Fig. 1b). These observations indicate that the F-actin bridges assemble between 12 and 24 hours after TAM treatment and suggest that their assembly is only transient. Because, the assembly of F-actin bridges is concomitant with the differentiation of a pool of CSCs, expressing low levels of CD24 (CD24^{low}) and capable of forming mammospheres⁷, my observations suggest that F-actin bridge assembly is involved in CSC differentiation taking place during oncogenic transformation.

To get insight on the mechanism by which the F-actin bridges assemble and disassemble, I quantified the number of bridges between two ER-Src cells during the 36 hours of TAM treatment. I defined two groups: cells interconnected by 1 to 4 bridges and those that were interconnected by 5 to 8 bridges. If the number of bridges is maintained constant over time, this would suggest that bridges formed between two cells assemble and disassemble at the same time. In contrast, if the numbers of bridges vary with time, this would suggest that the bridges formed between two cells assemble and disassemble gradually. At 4 and 12 hours after TAM treatment, interconnected cells were bound to each other by 1 to 4 F-actin bridges (Fig. 1c), while none had 5 to 8 bridges (Fig. 1d). Later, at 24 and 36 hours, most cells were bound to each other by 1 to 4 bridges, however, 1/5 were interconnected by 5 to 8 bridges (Fig. 1c,d). Although the percentage of interconnected cells decreased between 24 and 36 hours (Fig. 1b), the number of bridges per cells was not significantly different between these two time points. These observations suggest that the assembly of F-actin bridges takes place gradually between 12 and 24 hours, while their disassembly takes place simultaneously. Taken together, my observations suggest that Src-dependent cellular transformation involves the graduated assembly of F-actin bridges between 12 and 36 hours and their simultaneous disassembly after 24 hours.

While the presence of serum and growth factors is absolutely required for the growth and survival of EtOH-treated ER-Src cells, those that are treated with TAM proliferate and undergo cellular transformation in the absence of serum and growth factors. To test if ER-Src cells grown in the absence of serum and growth factors also assemble F-actin bridges 24 hours after TAM treatment, I stained ER-Src cells grown in medium free of supplements and treated with EtOH or TAM for 24 hours, with P-cadherin and E-cadherin, which

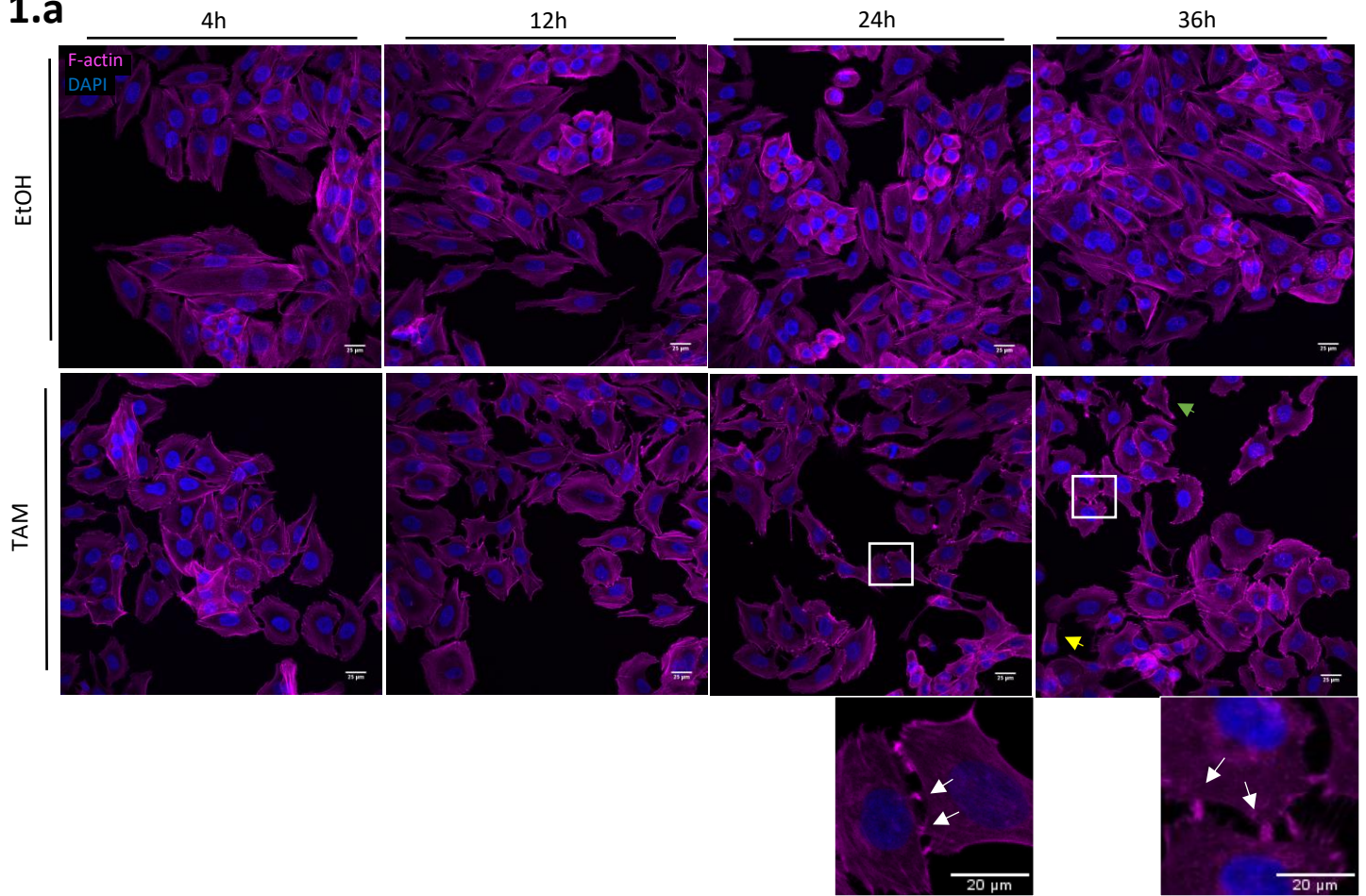
stain the cell population with a mesenchymal-like morphology (Figure 3 from Introduction), and with Phalloidin and DAPI. However, in these conditions, I could only observe rare F-actin bridges assembled between ER-Src cells treated with TAM for 24 hours. Nevertheless, most cells displayed an elongated or round morphology. Moreover, cells with high levels of both E- and P-cadherin failed to cluster together, which contrasted with EtOH-treated E/P-cadherin positive-cells, which appeared to adhere to each other (Supplementary Fig. a). Thus, the presence of serum and growth factors could speed up the timing of cellular transformation. To determine if TAM-treated ER-Src cells grown in the absence of serum and growth factors assemble the F-actin bridges earlier, I looked for the presence of F-actin bridges in these cells 12 hours after treatment. However, at this time point, ER-Src cells did not show either F-actin bridges connecting cells with each other (Supplementary Fig. a). These observations suggest that the assembly and disassembly of the F-actin bridges could be more transient in the absence of serum and growth factors.

2. Tpm1.6/1.7, as well as γ - and β -actin, localizes to F-actin bridges in ER-Src treated cells with TAM for 24 hours.

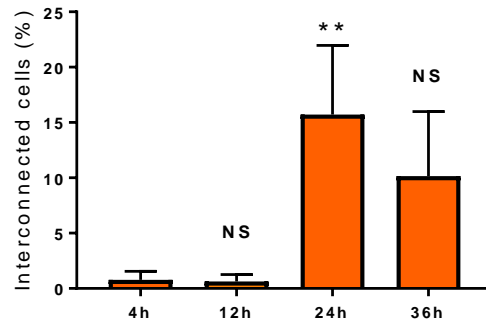
An increasing number of evidence indicates that actin filaments contain functional information, which predisposes them to perform specialized functions⁷³. To get insight on the role of F-actin bridges during cellular transformation, I searched for crucial components of these F-actin structures that could confer them specialized functional properties. Among those, tropomyosin (Tpm) isoforms, which form continuous polymers running along actin filaments, are good candidates⁷³. Several studies have established that Tpm isoforms are sensitive markers of the transformed state of a cell since the downregulation of heavy molecular weight (HMW) Tpm and the upregulation of low molecular weight (LMW) Tpm are associated to oncogenic transformation⁴⁶. Therefore, I tested if specific Tpm isoforms are associated to the assembly of the transient F-actin bridges in TAM-treated ER-Src cells by staining ER-Src cells treated with EtOH or TAM for 24 hours with antibodies specific to Tpm isoforms. The anti-CG β 6 antibody is specific to the HMW Tpm 1.6 and Tpm 1.7^{70,74}, the anti- α /1b antibody is specific to the LMW Tpm 1.8 and Tpm 1.9⁶⁷, the anti- γ /9d antibody is specific to the LMW Tpm 3.1 and Tpm 3.2⁷⁵ and the anti- δ /9d antibody is specific to the LMW Tpm 4.2^{71,72}. Tpm 3.1/3.2 accumulated in large patches throughout the cell and around the nucleus in mesenchymal-like ER-Src cells treated with TAM for 24 hours (Fig. 1e, yellow arrow). These observations are in agreement with a role of the LMW Tpm 3.1 in oncogenic transformation, as this isoform has been shown to be required for the survival of neuroblastoma, for cell proliferation through the MAPK pathway and to be associated with cell migration^{47,48}. However, Tpm 3.1/3.2 did not localize in F-actin bridges. Antibodies against Tpm 4.2 and Tpm 1.8/1.9 did not either stain F-actin bridges or other cell structures in EtOH- or TAM-treated ER-Src cells. Only the antibody against Tpm 1.6/1.7 was found to stain F-actin bridges (Fig. 1e, white arrows). Tpm 1.7 has been found to bind fascin⁴¹. Fascin is a protein tightly associated with stable F-actin filaments like filopodia and has been found upregulated in later stage breast cancer⁷⁶ and involved in CSC maintenance⁴³. Therefore, my observations suggest that the F-actin bridges could be involved in promoting the emergence of a CSC population and that the accumulation of Tpm 3.1 could promote the proliferation and/or migration of TAM-treated ER-Src cells.

Like tropomyosin isoforms, actin isoforms also play distinct cellular functions. β -actin was shown to promote cell growth and cell migration³⁴, while γ -actin was shown to have a tumor suppressor effect by reducing the mitotic arrest of cancer cells³⁵. Therefore, I stained ER-Src cells treated with TAM for 24 hours with antibodies specific against these actin isoforms. Both, γ - and β -actin localized at F-actin bridges (Fig. 1f, white arrows). Taken together, these observations suggest that Tpm1/6/1.7 could affect the assembly of F-actin bridges formed of γ - and β -actin in order to initiate a CSC program.

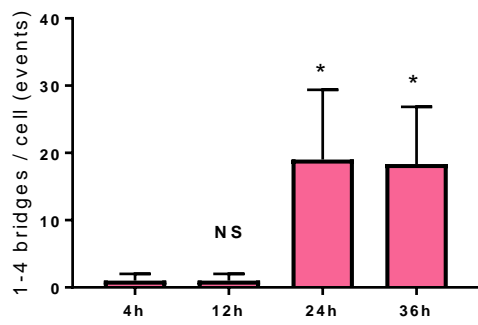
1.a



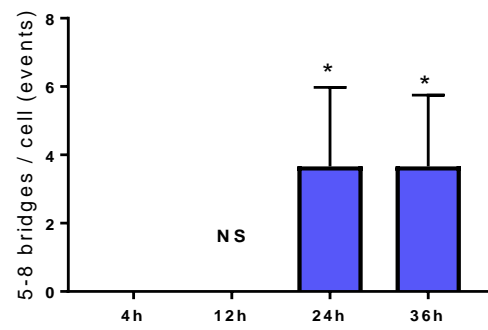
1.b



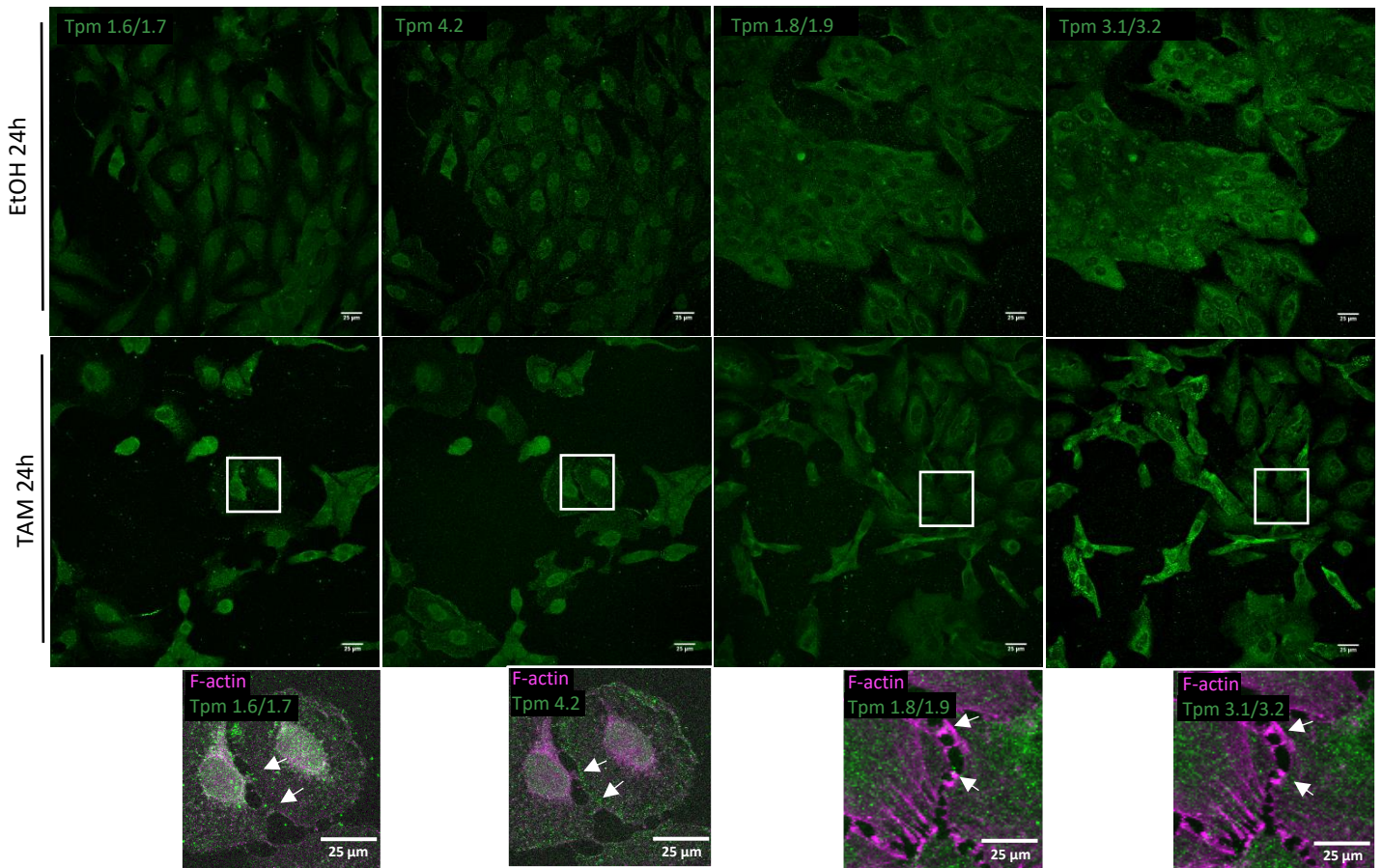
1.c



1.d



1.e



f

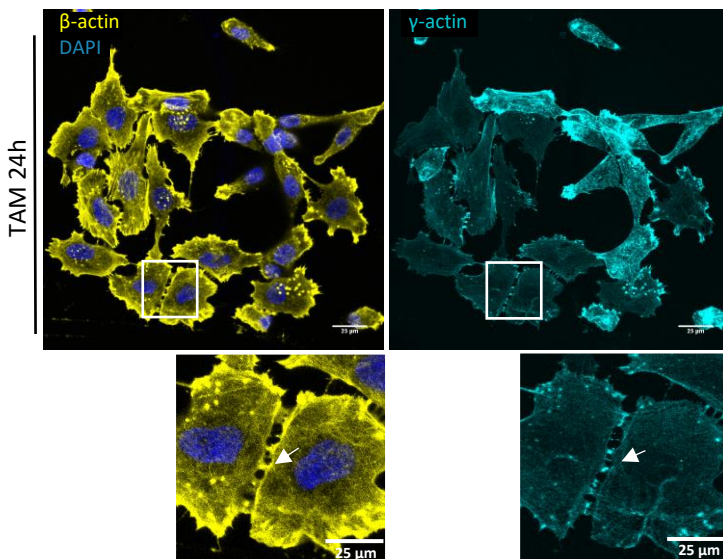


Figure 1: F-actin bridges are transiently assembled in TAM-treated ER-Src cells at 24 hours and accumulate Tpm1.6/1.7, γ - and β -actin. (a) Confocal images of ER-Src cells treated with EtOH or TAM for 4, 12, 24 or 36 h, stained with Phalloidin (magenta) to mark F-actin and DAPI (blue). (b) Percentage of ER-Src cells connected by F-actin bridges (interconnected cells), treated with TAM for 4, 12, 24 or 36 h. P-values for 12h and 24h were calculated comparing with the 4h timepoint. P-value for 36h was calculated comparing with the 24h timepoint. (c, d) Number of interconnected ER-Src cells, treated with TAM for 4, 12, 24 or 36 h with 1-4 bridges or 5-8 bridges. Quantifications are from three biological replicates with an average of 10 images per treatment for each replicate. Error bars indicate standard deviation.; NS indicates non-significant, * $P < 0.05$; ** $P < 0.001$. Statistical significance was calculated using one-way ANOVA. (e) Confocal images of ER-Src cells treated with EtOH or TAM for 24h, stained with anti-Tpm4.2 (green) and anti-Tpm1.6/1.7 (green), or anti-Tpm1.8/1.9 (green) and anti-Tpm3.1/3.2 (green) and with Phalloidin (magenta) to mark F-actin. Cropped images of F-actin bridges zoomed. (f) Confocal images of ER-Src cells treated with TAM for 24h, stained with anti- γ - (cyan), β -actin (yellow) and DAPI (blue). Scale bars represent 25 μm . White arrowheads indicate F-actin bridge.

3. ARPC5 localizes with ARPC5L at F-actin bridges in ER-Src cells, 24 hours after TAM treatment.

To determine if ARPC5 accumulates at F-actin bridges, I treated cells with EtOH or TAM for 4, 12, 24 and 36 hours and stained cells for both ARPC5 subunits (ARPC5 and ARPC5L). In EtOH treated cells, ARPC5 localized in the cytoplasm, with a stronger accumulation around the nucleus at all time points analyzed (Fig. 2a), while ARPC5L localized more ubiquitously in the cell cytoplasm. When ER-Src cells were treated with TAM for 4 or 12 hours, ARPC5 and ARPC5L maintained their cytoplasmic localization. However, at 24 and 36 hours after TAM treatment, cells bound to each other by F-actin bridges re-localized ARPC5 and ARPC5L to these bridges. In addition, both isoforms colocalized in dots within the cells, reminiscent to podosomes (Fig. 2a, yellow arrows). These observations showed that both ARPC5 subunits accumulate at F-actin bridges (Fig. 2a, white arrows), which suggests that both ARPC5 subunits are involved in F-actin bridge assembly.

I also analyzed the subcellular localization of ARPC5 and ARPC5L in ER-Src cells treated with TAM for 24 hours and grown in the absence of serum and growth factors. The previous ubiquitously ARPC5L cellular expression changed to an accumulation around the nucleus in only a small cell population. On the other hand, ARPC5 expression was maintained in most cells around the nucleus (Supplementary Fig.b). These observations suggest that the absence of serum and growth factors affect the assembly of the F-actin bridges, as well as the distribution of ARPC5 and ARPC5L in the cell, therefore, suggesting that growth conditions can alter F-actin bridge assembly dynamics by changing the ARPC5 and ARPC5L cellular subcellular localization.

4. Unlike ARPC5L, ARPC5 levels are not altered in ER-Src cells during the 36 hours of TAM treatment.

In addition, to accumulate in F-actin bridges, previous observations show that ARPC5L protein levels increase in TAM-treated ER-Src cells (M. Araujo, unpublished observation). This suggests that high levels of ARPC5L could be required to assemble the F-actin bridges, which in turn, would be involved in specifying a CSC fate. If ARPC5, which also localizes to the F-actin bridges, acts redundantly with ARPC5L in F-actin bridge assembly, ARPC5 levels could also increase in TAM-treated ER-Src cells. In contrast, if ARPC5 counteracts ARPC5L in F-actin bridge assembly, the cellular transformation could be associated with a reduction in ARPC5 levels. Therefore, I analyzed ARPC5 protein levels by Western Blot in ER-Src cells treated with EtOH or TAM for 4, 12, 24 and 36 hours (Fig. 2b). As expected, when normalized to treatment with EtOH at the same time points, TAM treatment potentiated the levels of the phosphorylated form of ER-Src (ER-pSrc) in a stepwise manner (Fig. 2c). Moreover, TAM treatment triggered the phosphorylation of endogenous Src (pSrc) (Fig. 2b). Quantifications of the ratio of ARPC5 levels between TAM and EtOH showed that ARPC5 levels were not significantly different during the 36 hours of TAM treatment (Fig. 2d). These observations indicate that ARPC5 levels are not affected during the transformation of the TAM-treated ER-Src cell line. This does not allow me to speculate on the role of ARPC5 in F-actin bridge assembly and in cellular transformation.

2.a

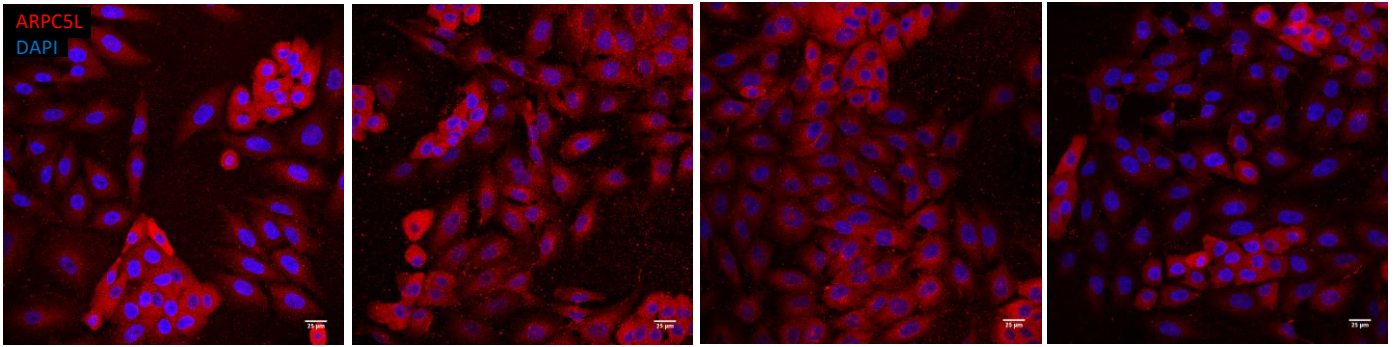
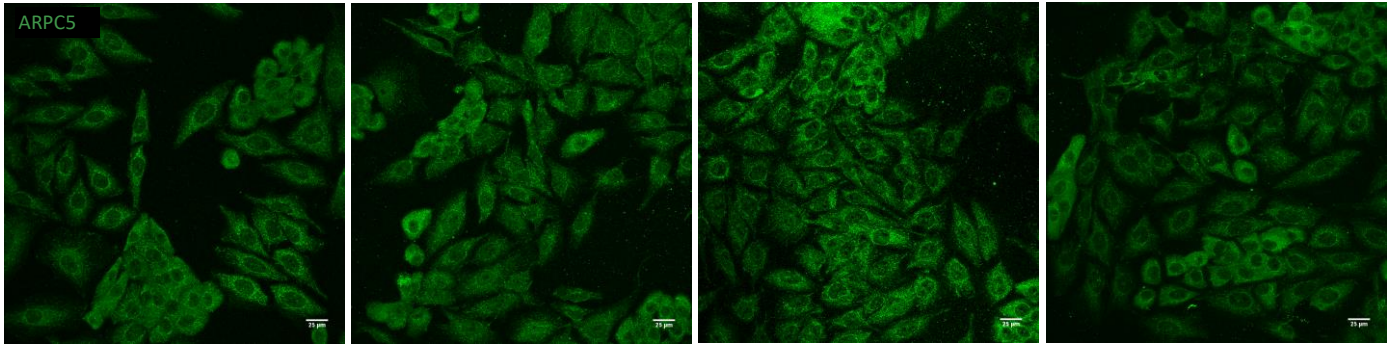
4h

12h

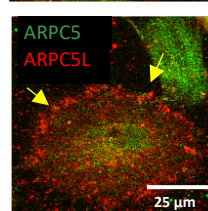
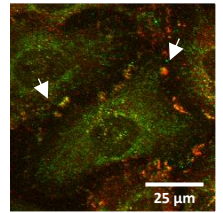
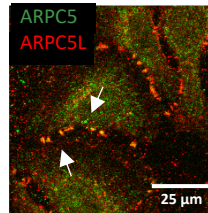
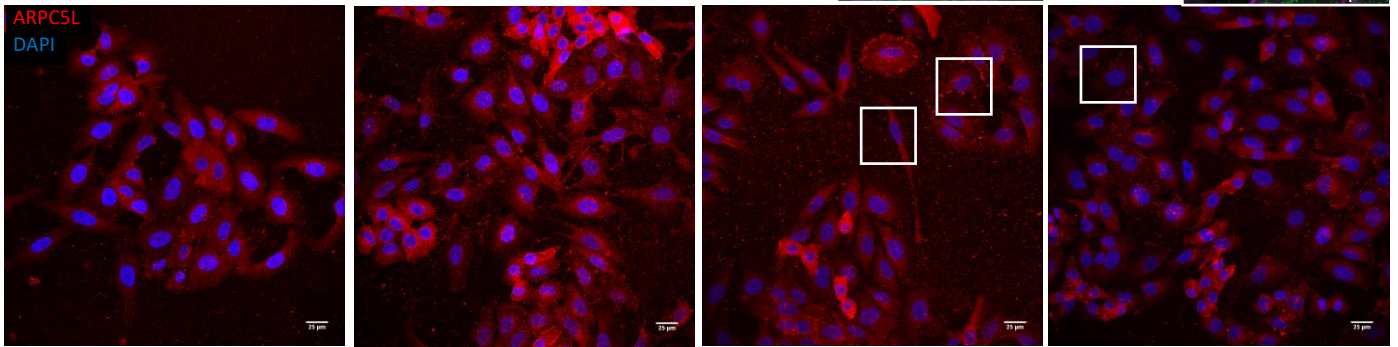
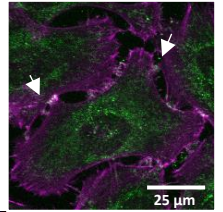
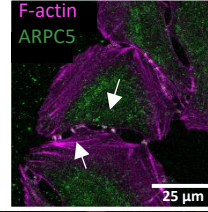
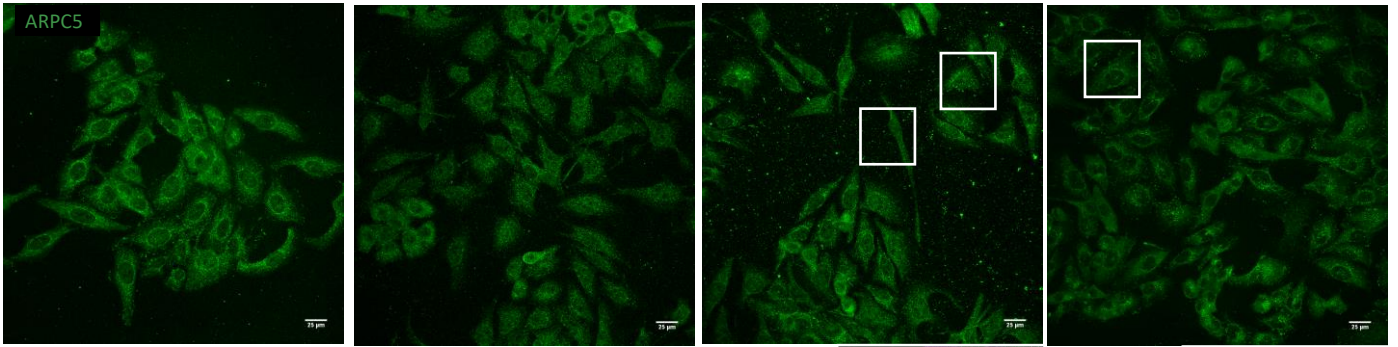
24h

36h

EtoH



TAM



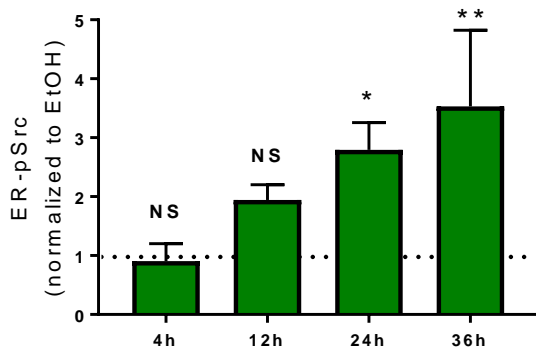
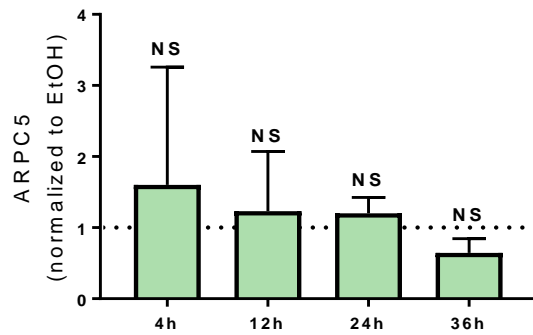
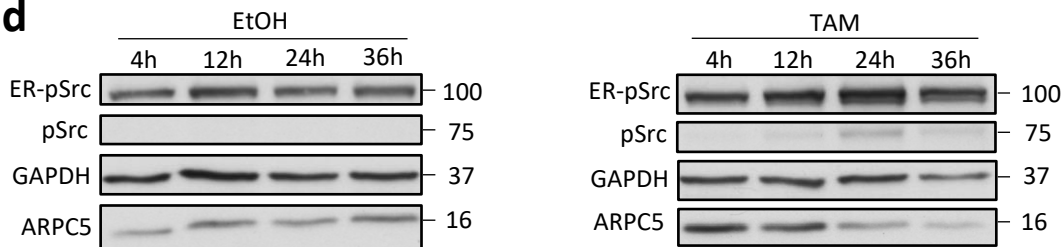
2.b**2.c****2.d**

Figure 2: ARPC5 localizes to the transient F-actin bridges but its expression levels are not altered in ER-Src cells during the 36 hours of TAM treatment. (a) Confocal images of ER-Src cells treated with EtOH or TAM for 4, 12, 24 or 36 h, stained with anti-ARPC5 (green), anti-ARPC5L (red), DAPI (blue) and Phalloidin (magenta) to mark F-actin. Cropped images of F-actin bridges zoomed. Scale bars represent 25 μ m. White arrowhead indicates F-actin bridges. (b) Western blots on protein extracts from ER-Src cells treated with EtOH or TAM for the same time points, blotted with anti-pSrc, which reveals ER-pSrc or endogenous pSrc, anti-GAPDH and anti-ARPC5. (c,d) Ratio of ER-pSrc (c) and ARPC5 (d) levels between TAM- and EtOH-treated ER-Src cells for the same time points, normalized to GAPDH. Quantifications are from three biological replicates. Error bars indicate standard deviation.; NS indicates non-significant, * $P < 0.05$; ** $P < 0.001$. Statistical significance was calculated using one-way ANOVA and by comparing the protein levels obtained in the TAM treatment with the protein levels obtained in the EtOH treatment.

5. ARPC5 could be required to assemble the F-actin bridges 24 hours after TAM treatment.

Although ARPC5 levels were not significantly altered in ER-Src cells during the 36 hours of TAM treatment, I analyzed if ARPC5 was required to assemble the F-actin bridges 24 hours after TAM treatment. To do so, I inhibited ARPC5 function using a small interfering RNA complementary to ARPC5 messenger RNA (siARPC5). As a control, I transfected cells with Scrambled RNA (siScr), which does not have a specific target. Cells transfected with siARPC5, to deplete ARPC5 expression, or siScr, to see if the knockdown conditions alone are altering the ARPC5 expression, were then treated with EtOH or TAM for 24 hours. To confirm that ARPC5 levels were reduced in cells transfected with siARPC5 and that TAM treatment increases the levels of ER-pSrc, I analyzed ARPC5 protein levels and levels of phosphorylated Src by Western Blot (Fig. 3d). As expected, cells treated with TAM increased the levels of ER-pSrc and triggered the phosphorylation of endogenously expressed Src in siScr- and siARPC5-expressing cells, confirming that ER-Src cells respond to TAM treatment. Quantification of ARPC5 protein levels showed a substantial decrease to 87 % in siARPC5-expressing cells in both EtOH- and TAM-treated ER-Src cells (Fig. 3d). I then

tested the effect of knocking down ARPC5 on the assembly of F-actin bridges induced by Src activation. ER-Src cells, transfected with siScr or siARPC5 and treated with either EtOH or TAM, were stained with Phalloidin and with anti-ARPC5L, to mark the F-actin bridges, and with anti-E-cadherin, an apical polarity and epithelial marker. Like EtOH-treated ER-Src cells transfected with siScr, EtOH-treated ER-Src cells knocked down for ARPC5 did not show interconnected cells through F-actin bridges (Fig. 3a,b,e). Knocking down ARPC5 in TAM-treated ER-Src cells reduced the average number of interconnected cells compared to the one observed in TAM-treated ER-Src cells transfected with shScr. However, this reduction was not significant (Fig. 3a,b,c). However, based on the interconnected cell population frequency acquired after 24h of TAM treatment, which reached approximately 15% of the total cell population, we can suggest that ARPC5 could be required to assemble F-actin bridges, since in knockdown conditions for ARPC5 after 24h of TAM treatment the interconnected cell population only reached 5%, approximately.

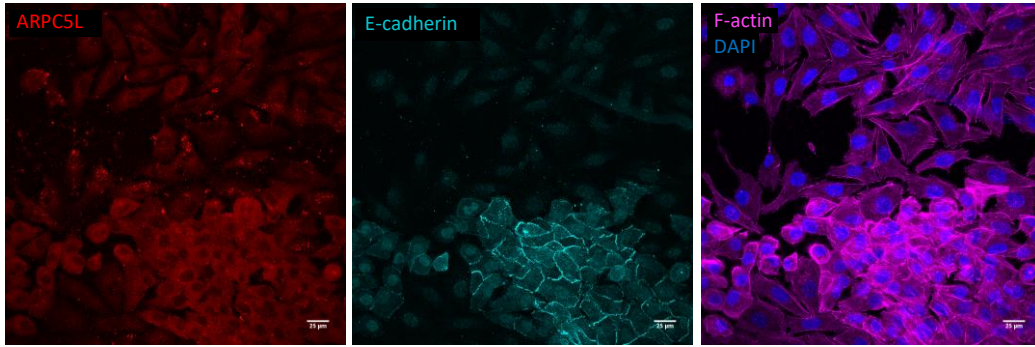
6. ARPC5 does not alter the frequency of epithelial and mesenchymal cell populations in ER-Src cells treated with TAM for 24 hours.

In addition to inducing the emergence of a population of cells interconnected to each other through F-actin bridges, observations suggest that the treatment of ER-Src cells with TAM for 24 hours reduces the number of cells with an epithelial phenotype, while inducing the emergence of a population of cells with a mesenchymal-like morphology (Fig. 1a.). Interestingly, during tumor progression epithelial cells undergo EMT (epithelial-mesenchymal transition), in which they acquire mesenchymal traits and migrating abilities, losing cell polarity, suppressing epithelial cell markers and upregulating mesenchymal ones. Moreover, partial EMT, in which cells do not fully acquire a mesenchymal phenotype and display both epithelial and mesenchymal properties, has been demonstrated to provide cancer cells with the potential to be CSCs^{77,78}. Therefore, the mesenchymal cell population observed 24 hours after TAM treatment could correspond to a CSC pool and, if so, interconnected cells could be controlling their formation through F-actin bridge assembly. To determine if ARPC5 affects the number of cells with an epithelium or a mesenchymal phenotype, ER-Src cells transfected with siARPC5 or siScr and treated with EtOH or TAM for 24 hours, were stained with Phalloidin, anti-ARPC5L, and anti-E-cadherin. I then quantified the proportion of different cell populations. Cells were identified as mesenchymal based on their elongated morphology with ARPC5L ubiquitously in the cell and E-cadherin in the nucleus. In contrast, cells that were compacted with ARPC5L ubiquitously localized in the cytoplasm and E-cadherin at the membrane were identified as epithelial. Other cells that were geometrically shaped, expressing weak ARPC5L and E-cadherin levels were labeled as fibroblastic (Fig. 3c). Knocking down ARPC5 in ER-Src cells treated with EtOH did not alter the number of mesenchymal, epithelial or fibroblastic cells, compared to EtOH-treated cells transfected with shScr (Fig. 3a,b). Similarly, knocking down ARPC5 in TAM-treated cells did not alter the number of these cell populations (Fig. 3e,f,g) compared to TAM-treated ER-Src cells transfected with siScr. Unfortunately, the high standard deviations obtained point to the conclusion that the quantification process used was not appropriate to ascertain the cell number of these cell populations, which render these data inconclusive. However, this could also mean based on these observations that I am strictly selecting epithelial and mesenchymal cells, hence not being able to separate the populations indicative of a partial EMT, which display characteristics of both. Nevertheless, my data suggests that ARPC5 is not involved in EMT during Src-induced cellular transformation.

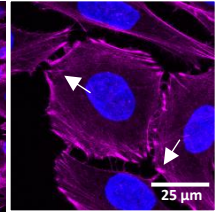
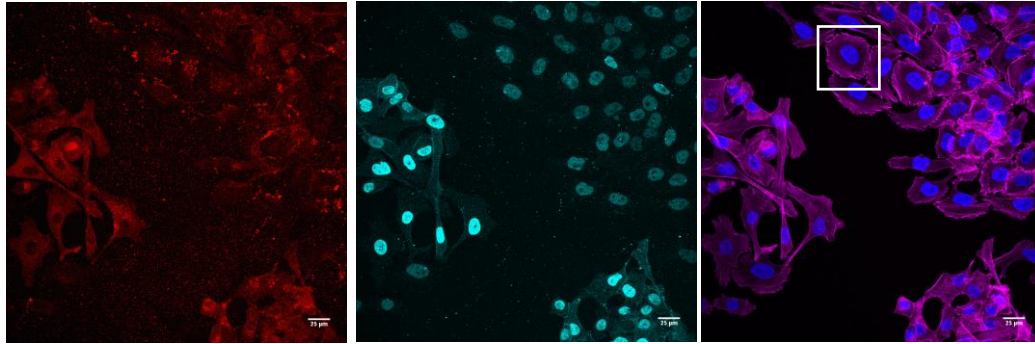
3.a

siScr

EtOH 24h



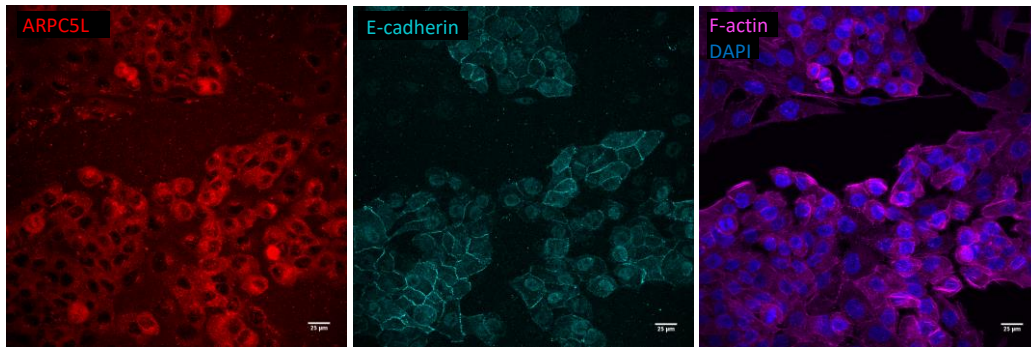
TAM 24h



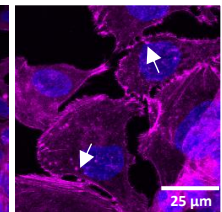
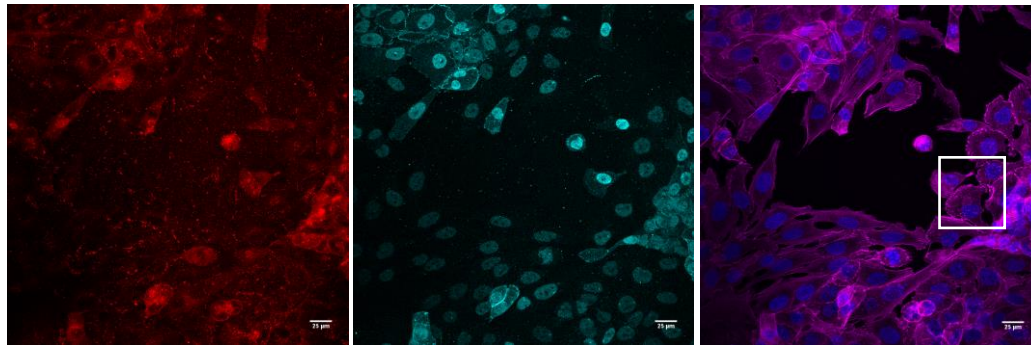
3.b

siARPC5

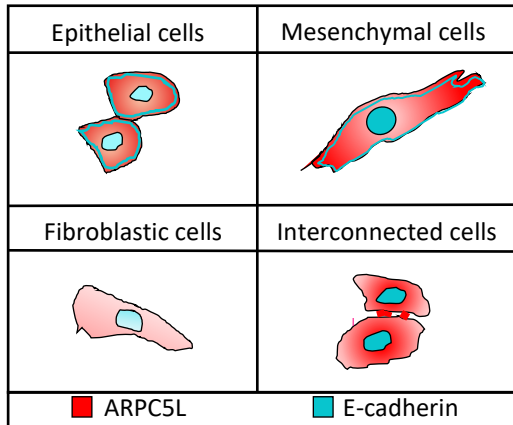
EtOH 24h



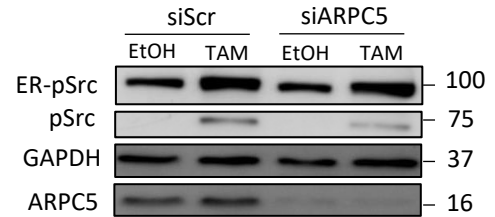
TAM 24h



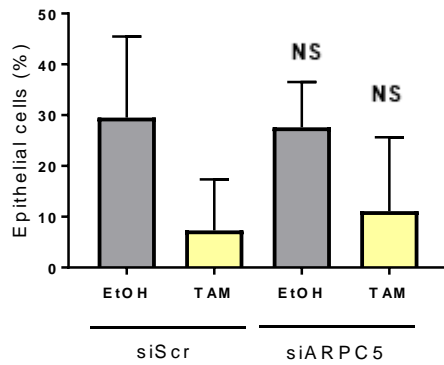
3.c



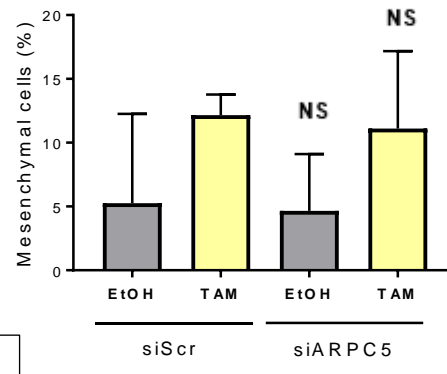
3.d



3.e

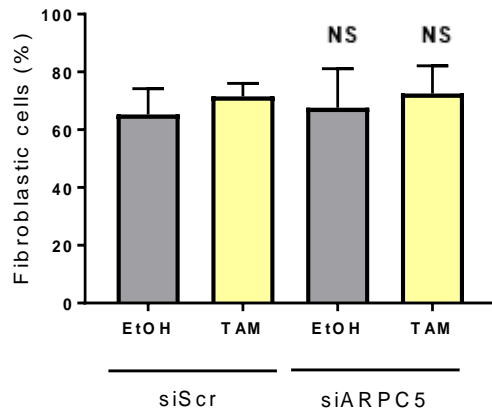


3.f



t=24h

3.g



3.h

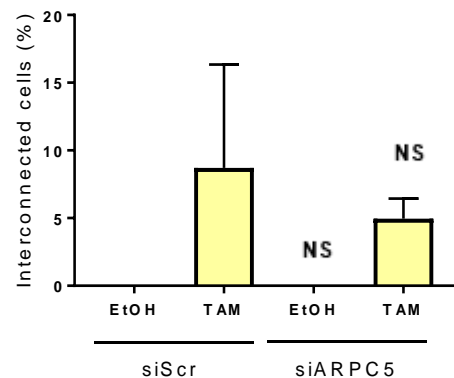


Figure 3: Knocking down ARPC5 did not alter the subcellular population frequency in ER-Src cells treated with TAM for 24 hours. (a) Confocal images of ER-Src cells expressing siScr (negative control) or (b) siARPC5 treated with EtOH or TAM for 24 h, stained with Phalloidin (magenta) to mark F-actin, DAPI (blue), anti-ARPC5L (red) and anti-E-cadherin (cyan). Scale bars represent 25 μ m. White arrowhead indicates F-actin bridges. Cropped images of F-actin bridges zoomed. (c) Schematic representation of distinct ER-Src cell populations identified upon EtOH or TAM treatments, based on ARPC5L/E-cadherin localization and cell morphology. (d) Western blots on protein extracts from ER-Src cells expressing siScr or siARPC5 treated with EtOH or TAM for 24 h, blotted with anti-pSrc, which reveals ER-pSrc and endogenous pSrc, anti-GAPDH and anti-ARPC5. (e, f, g, h) Percentage of interconnected (e) or epithelial (f) or mesenchymal (g) or fibroblastic (h) ER-Src cells, transfected with siScr or siARPC5 and treated with EtOH (grey bars) or TAM (yellow bars) for 24h. Quantifications are from two biological replicates with an average of 10 images per treatment for each replicate. Error bars indicate s.d.; NS indicates non-significant. Statistical significance was calculated using one-way ANOVA. P-values were calculated comparing EtOH treatments and comparing TAM treatments.

7. ARPC5 could increase the mammosphere-forming abilities of TAM-treated ER-Src cells.

Because ARPC5 was suggested to be involved in F-actin bridge assembly, which was also suggested to be associated with the acquisition of CSC properties, I analyzed if ARPC5 promotes stemness-like properties using mammosphere assays. This assay takes advantage of the anchorage-independent growth of stem cells that remain in suspension and form aggregates of acinar-like structures, therefore, allowing me to evaluate stemness properties, based on the size and frequency of these structures. I compared the mammosphere-forming abilities of ER-Src cells transfected with siScr or siARPC5 and treated with EtOH or TAM. I considered structures equal or superior to $45 \mu\text{m}^2$ to quantify Mammosphere-Forming-Efficiency (MFE). As expected, ER-Src cells expressing siScr and treated with TAM formed more mammospheres compared to ER-Src expressing siScr and treated with EtOH (Fig. 4a, b). Knocking down ARPC5 in TAM-treated ER-Src cells decreased their MFE compared to TAM-treated ER-Src cells transfected with SiScr (Fig. 4a, b). To confirm that TAM treatments induce the phosphorylation of ER-Src and endogenous Src, and to evaluate the levels of ARPC5 knocked down in cells transfected with siARPC5, I analyzed by Western Blot ER-pSrc, pSrc, and ARPC5 protein levels (Fig. 4c). Unfortunately, the levels of GAPDH used as loading control were too different between samples to confirm that TAM treatment increased ER-pSrc levels, while ARPC5L levels were decreased in cells transfected with siARPC5. Nevertheless, these observations suggest that ARPC5 could be required to promote stemness features in TAM-treated ER-Src cells.

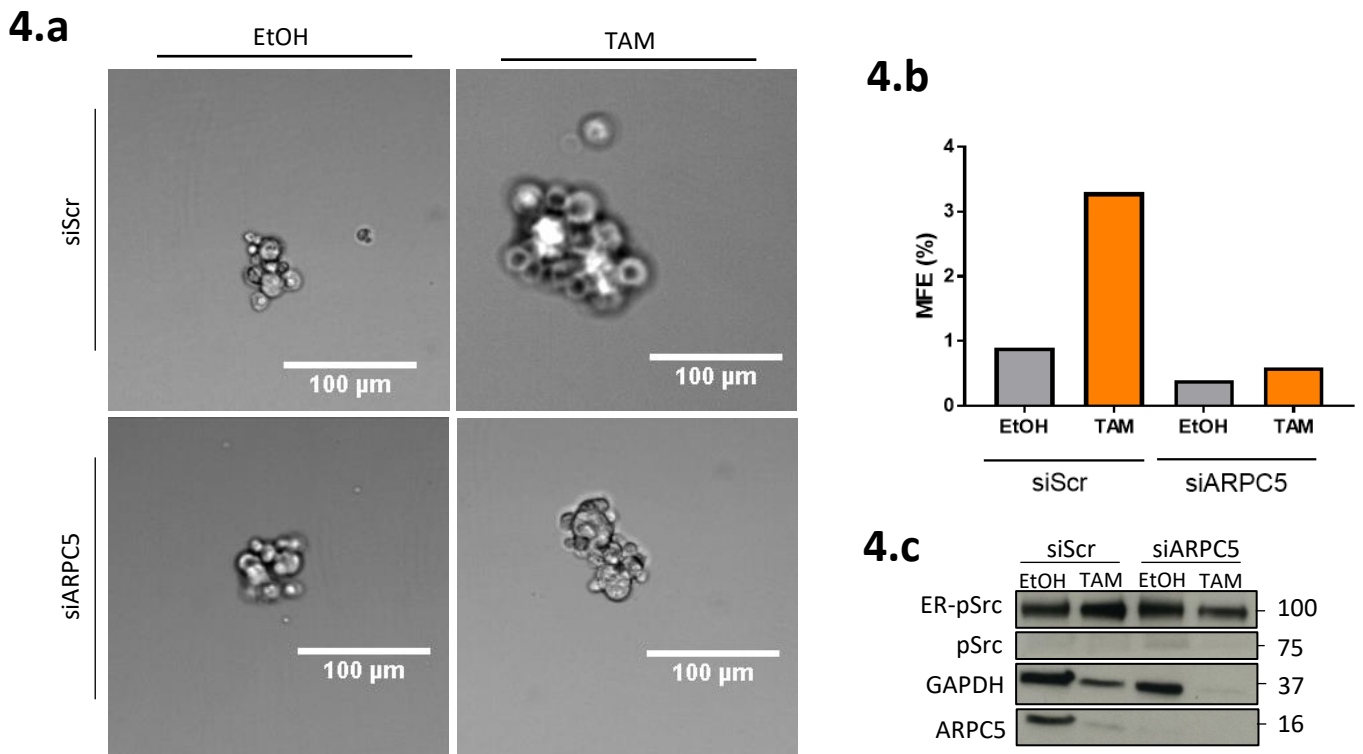


Figure 4: Knocking down ARPC5 reduces the mammosphere-forming efficiency of TAM-treated ER-Src cells. (a) 5-day cultures on Poly-HEMA of ER-Src cells treated with EtOH or TAM for 36 h, expressing siScr or siARPC5. Scale bars represent 100 μm . (b) Mammosphere-forming efficiency for the four experimental conditions in a. EtOH treatments (grey bars), TAM treatments (orange bars). (c) Western blots on protein extracts, collected before cell seeding for mammosphere formation, blotted with anti-pSrc, which reveals ER-pSrc and endogenous pSrc, anti-GAPDH and anti-ARPC5. Results are from one biological replicate.

DISCUSSION

1. F-actin bridges resemble Immunological Synapses and could act as “signaling platforms”.

Cell transformation induced by Src oncogene activation through TAM exposure led to the emergence of interconnected cells, characterized by the occurrence of F-actin bridges that connect neighboring cells. Over time, the percentage of the interconnected cell population dynamically changed, increasing between 12h and 24h after TAM treatment, which points for F-actin bridges being assembled at these time points, and suggests that they are specific of a transformed state.

Similar actin structures like midbodies, for example, are actin structures that occur in somatic cells as a consequence of cell division at the end of cytokinesis and mark the site where the mother cell is abscised to form individual daughter cells. This temporary connection is known to allow the passage from one cell to another of membrane-trafficking proteins, protein kinases, actin- and microtubule-associated proteins^{79,80}, which could suggest a similar role for F-actin bridges. Also, midbodies can alter their fate to become permanent intercellular bridges, in germ cell cytokinesis, and can transport even larger particles, like mitochondria⁸¹. Unlike F-actin bridges, cell division produces only one midbody for every two cells, while TAM-treated ER-Src cells assemble multiple F-actin bridges. This does not support the notion that F-actin bridges are midbodies resulting from cell division.

On the other hand, F-actin bridges could arise like tunneling nanotubes, in which migrating cells through thin cytoplasmic projections – filopodia – extend beyond the leading edge and form connections. Once filopodia reach a neighboring cell, they convert into a bridge connecting both cells. Another way for tunneling nanotubes to form is through membrane dislodgment of a thin membrane thread. They function as “highways” capable of transporting organelles, vesicles and cell signals between immune cells, like B cells and macrophages but were also found in cells from other tissues⁸². Interestingly, it has been proposed that tunneling nanotubes are the equivalent structure found in the *Drosophila* wing imaginal disc, called cytoneme, that extends between morphogen-producing cells that determine the fate of their target cells⁸³, which could also be the function played by F-actin bridges in cell transformation. However, they are improbable to be tunneling nanotubes since these structures usually occur singularly and are thinner and longer morphologically.

Alternatively, F-actin bridges could result from the assembly of a similar structure highly involved in cell-to-cell signaling: the immunological synapse. This structure is known to assemble and disassemble in short periods of time, over the course of minutes to hours. In this direct cell interaction, the actin cytoskeleton of a migrating cell rearranges itself so that their cell receptors can engage with the ligands of a neighboring cell. To assist in pulling both cells together, the Immunological Synapse has adhesion molecules, such as integrins and cadherins, surrounding the T-cell receptors⁸⁴. My data argues for the possibility that F-actin bridges are reminiscent to Immunological Synapses, by showing concentrated regions of F-actin clusters that are assembled and disassembled intercellularly over the course of hours. The observations showing F-actin bridges being assembled in the course of a few hours are in agreement with the signaling function of Immunological Synapses, because F-actin bridges could be assembled like IS are to allow signal transfer and later disassemble. The observed F-actin bridges could be reminiscent of the occurred cell process. In addition, F-actin bridges express both ARPC5 and ARPC5L isoforms and could require ARPC5 for their assembly, which points to the involvement of the Arp2/3 complex activity in their assembly. Furthermore, cell transformation occurring in conditions of serum and growth factors absence originated rare interconnected cells by F-actin bridges and detached mesenchymal-like cells with E-cadherin and P-cadherin at their cell membranes. These observations are in agreement with previous studies that have shown that TAM-treated ER-Src cells acquire self-sufficiency in growth properties prior to migrating abilities⁴⁹, which could be associated with a mesenchymal-like phenotype. However, the hypothesis that another pathway for cell

transformation is taking place, which would not include F-actin bridge assembly, cannot be ruled out. Therefore, F-actin bridges could be associated with “signaling platforms”, which would appear at a specific transformed cell state in breast cancer tumor progression.

2. ARPC5 and ARPC5L could play opposite functions on F-actin bridge assembly.

The actin polymerization activity of Arp2/3 complex is most likely associated with F-actin bridges since ARPC5 and ARPC5L are located at F-actin bridges and since ARPC5 expression could be required for their assembly. However, ARPC5 protein levels were found to be stable throughout cell transformation. On the other hand, ARPC5L protein levels show a different expression trend for ARPC5L, with increasingly higher protein levels over time (M. Araujo, unpublished observation). Arp2/3 complexes containing ARPC5 or ARPC5L isoforms have been described in the formation of actin-based structures, such as viral actin tails and invadopodia, where ARPC5 absence promoted the assembly of both structures and the opposite was observed when ARPC5L was lacking⁶¹. These studies suggest that depending on the isoform, the Arp2/3 efficiency at polymerizing F-actin bridges is affected and supports the hypothesis that ARPC5 and ARPC5L should play opposite cell functions. Therefore, if ARPC5 promotes F-actin bridge assembly then ARPC5L could inhibit F-actin bridge occurrence, which is in agreement with the observed decrease in the interconnected cell population being concomitant with the increase of ARPC5L protein levels. In addition, since ARPC5 protein levels are kept stable throughout cell transformation, which is not true for ARPC5L, this points to ARPC5 activity being muted when ARPC5L activity takes over.

3. ARPC5 could promote Cancer Stem Cell features through F-actin bridge assembly.

My observations suggest that ARPC5 could promote the acquisition of CSC properties of transformed cells and that ARPC5 could also be required to form F-actin bridges. Previous observations showed that F-actin bridge assembly is concomitant with differentiation of a CSC pool⁷ and my data further suggests that ARPC5 could be necessary for F-actin bridge assembly and for the acquisition of CSC properties, which suggests that ARPC5 could assist in F-actin bridge assembly in order to trigger the CSC pool differentiation. Furthermore, ARPC5 was already shown to contribute to cell migration and invasion^{62,63}, cell behaviors associated with EMT. Since a partial EMT has been demonstrated to provide cancer cells with the potential to be CSCs^{77,78}, this further suggests that ARPC5 is involved in CSC property acquisition.

Contrarily, ARPC5L by inhibiting F-actin bridge assembly could inhibit by consequence the acquisition of CSC properties. However, previous studies found ARPC5L to contribute for tumor cell invasion since it is associated with invadopodia assembly. These observations also agree with the observations of ARPC5L overexpression during cell transformation being concomitant with an increase of mesenchymal cells, which could indicate that these cells went through a partial EMT, that could lead to CSC property acquisition, hence, suggesting that ARPC5L could also play a role in promoting the CSC program. Therefore, ARPC5 could promote CSC features through F-actin bridge assembly and ARPC5L, by inhibiting F-actin bridge assembly, could suppress CSC property acquisition. However, later during transformation ARPC5L could also be favoring the CSC program by regulating other cell feature besides F-actin bridge assembly.

4. Model: ARPC5-containing F-actin bridges could assist in intercellular communication to trigger the CSC program.

Transformed cells at 24 hours of induced cell transformation could assemble F-actin bridges, in order to contact with each other through “signaling platforms” to trigger the CSC program, thus promoting the downstream appearance of CSC’s. This intercellular connection could be based on cell receptors and stabilized through adhesion molecules and several F-actin bridges assembled with the actin polymerization activity of the ARPC5-rich Arp2/3 complexes. Supposing that these cell receptors of the signal-sending cell engage with the correspondent transmembrane ligands of the target cell, they can change the expression profile and trigger EMT and the CSC program on that cell, which could lead to the gain of migrating abilities later^{77,78}. The cell receptors in the signal-sending cell are likely of the Notch family due to their association with the differentiation and self-renewal of breast cancer cells^{16,17} and since Tpm 1.7, which recruits fascin that plays a role in maintaining the CSC pool through Notch^{41,43}, was found to at F-actin bridges. Once the signal is transmitted, ARPC5L protein levels rise which could favor the “signaling platform” destruction by promoting F-actin disassembly. It has been demonstrated that F-actin polymerized by ARPC5L-containing Arp2/3 complexes is less stable and more vulnerable to depolymerizing proteins, when absent of stabilizing proteins, like cortactin. Thus, the cell could regulate the expression of these stabilizing proteins together in order to favor the depolymerization of the F-actin assembled by ARPC5L subunits without affecting the F-actin assembled by ARPC5 since the stabilizing proteins are unable to bind to them. Moreover, the way ARPC5L could interfere and overlap with the ARPC5 activity for F-actin bridge assembly is by competing with ARPC5 for the other subunits of the Arp2/3 complex, needed to achieve the actin polymerization activity, which agrees with the function specificity proposed for these isoforms^{60,61}.

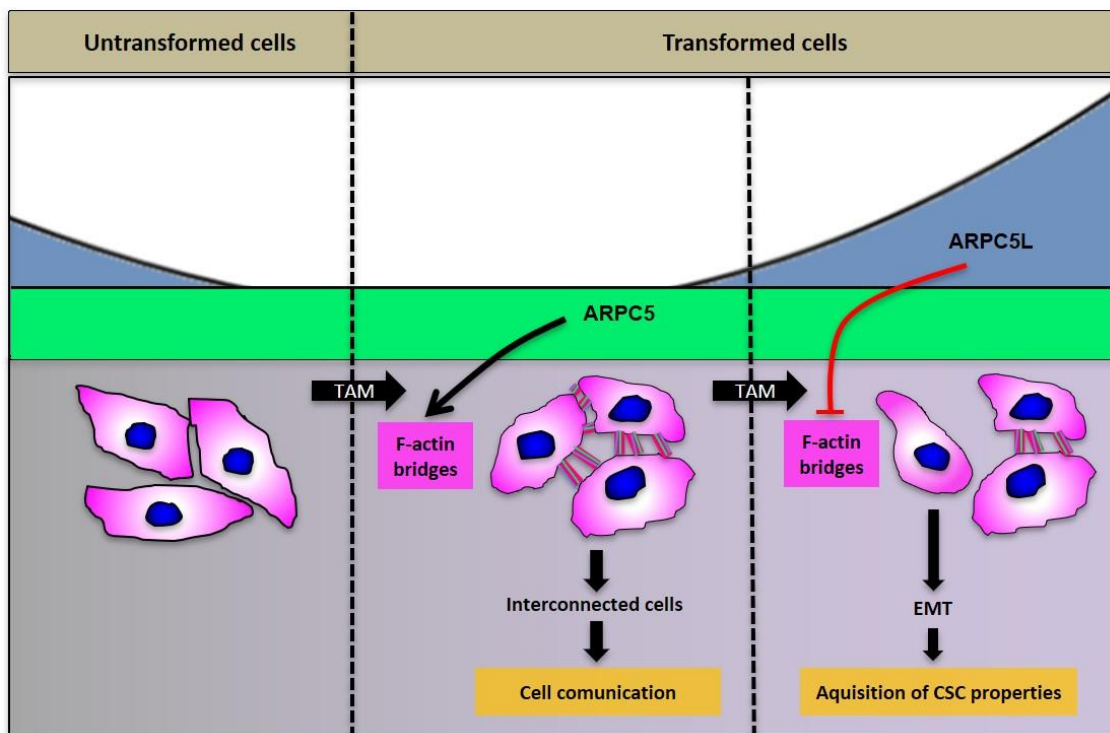
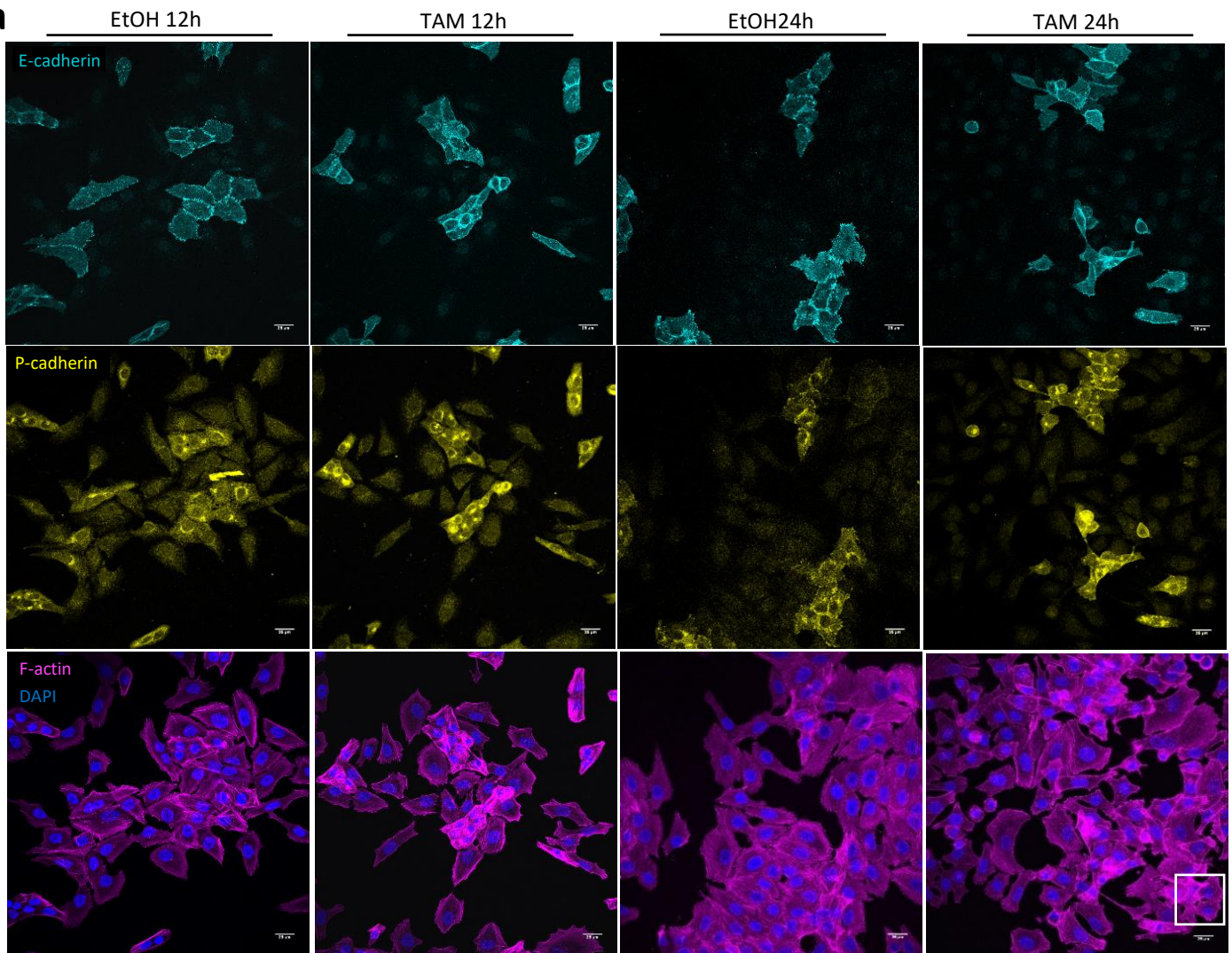


Figure 5: ARPC5 could assist in intercellular communication to trigger the acquisition of CSC properties. Early during cellular transformation, after tamoxifen administration, transformed cells could assemble F-actin bridges with ARPC5-containing Arp2/3 complexes when ARPC5L protein levels are low, leading to the formation of interconnected cells and allowing cell communication, which could trigger the CSC program. Later, ARPC5L protein levels increase, which could inhibit F-actin bridge assembly. Finally, cells could undergo EMT, predisposing cells to become CSCs.

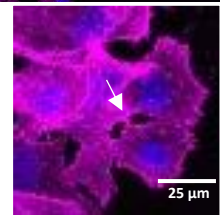
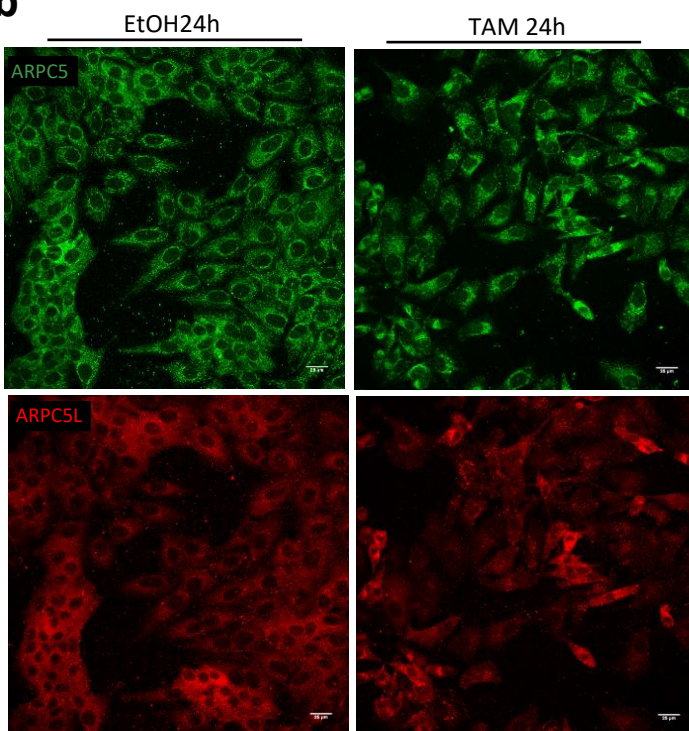
(inspired from Fig.9 of reference 49)

ANNEXES

S.a



S.b



Supplementary figure: Effect of supplementation-free growth conditions on TAM-treated ER-Src cells. (a) Confocal images of ER-Src cells treated with EtOH or TAM for 12 or 24 h, stained with anti-E-cadherin (cyan), anti-P-cadherin (yellow), DAPI (blue) and Phalloidin (magenta) to mark F-actin. (b) Confocal images of ER-Src cells treated with EtOH or TAM for 24 h, stained with anti-ARPC5 (green), anti-ARPC5L (red). Cropped image of F-actin bridges zoomed. Scale bars represent 25 μm . White arrowhead indicates F-actin bridges.

REFERENCES

1. WHO | Breast cancer: prevention and diagnosis. *WHO*. 2018. <http://www.who.int/cancer/prevention/diagnosis-screening/breastcancer/en/>. Accessed December 26, 2018.
2. Jandial R. *Metastatic Cancer: Clinical and Biological Perspectives*. Cardiff, UK: Landes Bioscience; 2013.
3. Li F, Tiede B, Massagué J, Kang Y. Beyond tumorigenesis: Cancer stem cells in metastasis. *Cell Res*. 2007;17(1):3-14. doi:10.1038/sj.cr.7310118
4. Bonnet D, Dick JE. Human acute myeloid leukemia is organized as a hierarchy that originates from a primitive hematopoietic cell. *Nat Med*. 1997;3(7):730-737. doi:10.1038/nm0797-730
5. Dallas NA, Xia L, Fan F, et al. Chemoresistant Colorectal Cancer Cells, the Cancer Stem Cell Phenotype and Increased Sensitivity to Insulin-like Growth Factor Receptor-1 Inhibition. 2009;69(5):1951-1957. doi:10.1158/0008-5472.CAN-08-2023.Chemoresistant
6. Bao S, Wu Q, McLendon RE, et al. Glioma stem cells promote radioresistance by preferential activation of the DNA damage response. *Nature*. 2006;444(7120):756-760. doi:10.1038/nature05236
7. Iliopoulos D, Hirsch HA, Wang G, Struhl K. Inducible formation of breast cancer stem cells and their dynamic equilibrium with non-stem cancer cells via IL6 secretion. *Proc Natl Acad Sci*. 2011;108(4):1397-1402. doi:10.1073/pnas.1018898108
8. Al-Hajj M, Wicha MS, Benito-Hernandez A, Morrison SJ, Clarke MF. Prospective identification of tumorigenic breast cancer cells. *Proc Natl Acad Sci*. 2003;100(7):3983-3988. doi:10.1073/pnas.0530291100
9. Meyer MJ, Fleming JM, Ali MA, Pesesky MW, Ginsburg E, Vonderhaar BK. Dynamic regulation of CD24 and the invasive, CD44posCD24negphenotype in breast cancer cell lines. *Breast Cancer Res*. 2009;11(6):23-31. doi:10.1186/bcr2449
10. Rappa G, Lorico A. Phenotypic characterization of mammosphere-forming cells from the human MA-11 breast carcinoma cell line. *Exp Cell Res*. 2010;316(9):1576-1586. doi:10.1016/j.yexcr.2010.01.012
11. Pece S, Tosoni D, Confalonieri S, et al. Biological and Molecular Heterogeneity of Breast Cancers Correlates with Their Cancer Stem Cell Content. *Cell*. 2010;140(1):62-73. doi:10.1016/j.cell.2009.12.007
12. Vieira AF, Ricardo S, Ablett MP, et al. P-cadherin is coexpressed with CD44 and CD49f and mediates stem cell properties in basal-like breast cancer. *Stem Cells*. 2012;30(5):854-864. doi:10.1002/stem.1075
13. Paredes J, Albergaria A, Oliveira JT, Jeronimo C, Milanezi F, Schmitt FC. P-cadherin overexpression is an indicator of clinical outcome in invasive breast carcinomas and is associated with CDH3 promoter hypomethylation. *Clin Cancer Res*. 2005;11(16):5869-5877. doi:10.1158/1078-0432.CCR-05-0059
14. Imai K, Hirata S, Irie A, et al. Identification of a novel tumor-associated antigen, cadherin 3/P-cadherin, as a possible target for immunotherapy of pancreatic, gastric, and colorectal cancers. *Clin Cancer Res*. 2008;14(20):6487-6495. doi:10.1158/1078-0432.CCR-08-1086
15. Ribeiro AS, Sousa B, Carreto L, et al. P-cadherin functional role is dependent on E-cadherin cellular context: A proof of concept using the breast cancer model. *J Pathol*. 2013;229(5):705-718. doi:10.1002/path.4143
16. Hoey T, Yen WC, Axelrod F, et al. DLL4 Blockade Inhibits Tumor Growth and Reduces Tumor-Initiating Cell Frequency. *Cell Stem Cell*. 2009;5(2):168-177. doi:10.1016/j.stem.2009.05.019
17. Rosemarie C. D'Angelo, Maria Ouzounova, April Davis, Daejin Choi, Stevie M. Tchuenkam, Gwangil Kim, Tahra Luther1, Ahmed A. Quraishi1, Yasin Senbabaoglu4, Sarah J. Conley, Shawn G. Clouthier, Khaled A. Hassan1, Max S. Wicha1 and HK. Notch reporter activity in breast cancer cell lines identifies a subset of cells with stem cell activity. 2015;14(3):69-81. doi:10.1158/1535-7163.MCT-14-0228
18. Goley ED, Rammohan A, Znameroski EA, Firat-Karalar EN, Sept D, Welch MD. An actin-filament-binding interface on the Arp2/3 complex is critical for nucleation and branch stability. *Proc Natl Acad Sci*. 2010;107(18):8159-8164. doi:10.1073/pnas.0911668107
19. Dosremedios CG, Chhabra D, Kekic M, et al. Actin binding proteins: Regulation of cytoskeletal microfilaments. *Physiol Rev*. 2003;83(2):433-473. doi:10.1152/physrev.00026.2002
20. Xue C, Wyckoff J, Liang F, et al. Epidermal growth factor receptor overexpression results in

- increased tumor cell motility in vivo coordinately with enhanced intravasation and metastasis. *Cancer Res.* 2006;66(1):192-197. doi:10.1158/0008-5472.CAN-05-1242
21. Schulze ES, Blose SH. Passage of molecules across the intercellular bridge between post-mitotic daughter cells. *Exp Cell Res.* 1984;151(2):367-373. doi:10.1016/0014-4827(84)90387-2
 22. D. BM and fawcett. Studies on the fine structure of the mammalian testis. 1955;1.
 23. Onfelt B, Nedvetzki S, Yanagi K, Davis DM. Cutting Edge: Membrane Nanotubes Connect Immune Cells. *J Immunol.* 2004;173(3):1511-1513. doi:10.4049/jimmunol.173.3.1511
 24. Lu J, Zheng X, Li F, et al. Tunneling nanotubes promote intercellular mitochondria transfer followed by increased invasiveness in bladder cancer cells. *Oncotarget.* 2017;8(9):15539-15552. doi:10.18632/oncotarget.14695
 25. Dugina V, Zwaenepoel I, Gabbiani G, Clement S, Chaponnier C. - and -Cytoplasmic Actins Display Distinct Distribution and Functional Diversity. *J Cell Sci.* 2009;122(16):2980-2988. doi:10.1242/jcs.041970
 26. Krause M, Gautreau A. Steering cell migration: Lamellipodium dynamics and the regulation of directional persistence. *Nat Rev Mol Cell Biol.* 2014;15(9):577-590. doi:10.1038/nrm3861
 27. Cramer LP, Siebert M, Mitchison TJ. Identification of novel graded polarity actin filament bundles in locomoting heart fibroblasts: Implications for the generation of motile force. *J Cell Biol.* 1997;136(6):1287-1305. doi:10.1083/jcb.136.6.1287
 28. Hirata H, Tatsumi H, Sokabe M. Dynamics of actin filaments during tension-dependent formation of actin bundles. *Biochim Biophys Acta - Gen Subj.* 2007;1770(8):1115-1127. doi:10.1016/j.bbagen.2007.03.010
 29. Tojkander S, Gateva G, Lappalainen P. Actin stress fibers - assembly, dynamics and biological roles. *J Cell Sci.* 2012;125(8):1855-1864. doi:10.1242/jcs.098087
 30. Mattila PK, Lappalainen P. Filopodia: Molecular architecture and cellular functions. *Nat Rev Mol Cell Biol.* 2008;9(6):446-454. doi:10.1038/nrm2406
 31. Gimona M, Buccione R, Courtneidge SA, Linder S. Assembly and biological role of podosomes and invadopodia. *Curr Opin Cell Biol.* 2008;20(2):235-241. doi:10.1016/j.ceb.2008.01.005
 32. Comrie WA, Burkhardt JK. Action and traction: Cytoskeletal control of receptor triggering at the immunological synapse. *Front Immunol.* 2016;7(MAR):1-25. doi:10.3389/fimmu.2016.00068
 33. Gerdes HH, Rustom A, Wang X. Tunneling nanotubes, an emerging intercellular communication route in development. *Mech Dev.* 2013;130(6-8):381-387. doi:10.1016/j.mod.2012.11.006
 34. Bunnell TM, Burbach BJ, Shimizu Y, Ervasti JM. β -Actin specifically controls cell growth, migration, and the G-actin pool. *Mol Biol Cell.* 2011;22(21):4047-4058. doi:10.1091/mbc.E11-06-0582
 35. Po'uha ST, Kavallaris M. Gamma-actin is involved in regulating centrosome function and mitotic progression in cancer cells. *Cell Cycle.* 2015;14(24):3908-3919. doi:10.1080/15384101.2015.1120920
 36. Gunning PW, Hardeman EC, Lappalainen P, Mulvihill DP. Tropomyosin - master regulator of actin filament function in the cytoskeleton. *J Cell Sci.* 2015;128(16):2965-2974. doi:10.1242/jcs.172502
 37. Pan H, Gu L, Liu B, et al. Tropomyosin-1 acts as a potential tumor suppressor in human oral squamous cell carcinoma. *PLoS One.* 2017;12(2):1-13. doi:10.1371/journal.pone.0168900
 38. Tao T, Shi Y, Han D, et al. TPM3, a strong prognosis predictor, is involved in malignant progression through MMP family members and EMT-like activators in gliomas. *Tumor Biol.* 2014;35(9):9053-9059. doi:10.1007/s13277-014-1974-1
 39. Gimona M, Kazzaz J a, Helfman DM. Forced expression of tropomyosin 2 or 3 in v-Ki-ras-transformed fibroblasts results in distinct phenotypic effects. *Proc Natl Acad Sci U S A.* 1996;93(18):9618-9623. doi:10.1073/pnas.93.18.9618
 40. Tojkander S, Gateva G, Schevzov G, et al. A molecular pathway for myosin II recruitment to stress fibers. *Curr Biol.* 2011;21(7):539-550. doi:10.1016/j.cub.2011.03.007
 41. Creed SJ, Desouza M, Bamburg JR, Gunning P, Stehn J. Tropomyosin isoform 3 promotes the formation of filopodia by regulating the recruitment of actin-binding proteins to actin filaments. *Exp Cell Res.* 2011;317(3):249-261. doi:10.1016/j.yexcr.2010.10.019
 42. Al-Alwan M, Olabi S, Ghebeh H, et al. Fascin is a key regulator of breast cancer invasion that acts via the modification of metastasis-associated molecules. *PLoS One.* 2011;6(11). doi:10.1371/journal.pone.0027339
 43. Barnawi R, Al-Khaldi S, Majed Sleiman G, et al. Fascin Is Critical for the Maintenance of Breast Cancer Stem Cell Pool Predominantly via the Activation of the Notch Self-Renewal Pathway. *Stem Cells.* 2016;34(12):2799-2813. doi:10.1002/stem.2473

44. Temm-Grove CJ, Jockusch BM, Weinberger RP, Schevzov G, Helfman DM. Distinct localizations of tropomyosin isoforms in LLC-PK1 epithelial cells suggests specialized function at cell-cell adhesions. *Cell Motil Cytoskeleton*. 1998;40(4):393-407. doi:10.1002/(SICI)1097-0169(1998)40:4<393::AID-CM7>3.0.CO;2-C
45. Zucchi I, Bini L, Valaperta R, et al. Proteomic dissection of dome formation in a mammary cell line: role of tropomyosin-5b and maspin. *Proc Natl Acad Sci U S A*. 2001;98(10):5608-5613. doi:10.1073/pnas.091101898
46. Schevzov G, Kee AJ, Wang B, et al. Regulation of cell proliferation by ERK and signal-dependent nuclear translocation of ERK is dependent on Tm5NM1-containing actin filaments. *Mol Biol Cell*. 2015;26(13):2475-2490. doi:10.1091/mbc.E14-10-1453
47. Bach CTT, Creed S, Zhong J, et al. Tropomyosin Isoform Expression Regulates the Transition of Adhesions To Determine Cell Speed and Direction. *Mol Cell Biol*. 2009;29(6):1506-1514. doi:10.1128/MCB.00857-08
48. Lees JG, Ching YW, Adams DH, et al. Tropomyosin regulates cell migration during skin wound healing. *J Invest Dermatol*. 2013;133(5):1330-1339. doi:10.1038/jid.2012.489
49. Tavares S, Vieira AF, Taubenberger AV, et al. Actin stress fiber organization promotes cell stiffening and proliferation of pre-invasive breast cancer cells. *Nat Commun*. 2017;8(May). doi:10.1038/ncomms15237
50. Suraneni P, Rubinstein B, Unruh JR, Durnin M, Hanein D, Li R. The Arp2/3 complex is required for lamellipodia extension and directional fibroblast cell migration. *J Cell Biol*. 2012;197(2):239-251. doi:10.1083/jcb.201112113
51. Iwaya K, Norio K, Mukai K. Coexpression of Arp2 and WAVE2 predicts poor outcome in invasive breast carcinoma. *Mod Pathol*. 2007;20(3):339-343. doi:10.1038/modpathol.3800741
52. Semba S, Iwaya K, Matsubayashi J, et al. Coexpression of actin-related protein 2 and Wiskott-Aldrich syndrome family verproline-homologous protein 2 in adenocarcinoma of the lung. *Clin Cancer Res*. 2006;12(8):2449-2454. doi:10.1158/1078-0432.CCR-05-2566
53. Wang W, Wyckoff JB, Frohlich VC, et al. Single Cell Behavior in Metastatic Primary Mammary Tumors Correlated with Gene Expression Patterns Revealed by Molecular Profiling Single Cell Behavior in Metastatic Primary Mammary Tumors Correlated with Gene Expression Patterns Revealed by Molecular Pro. *Cancer Res*. 2002;62(21):6278-6288. <http://eutils.ncbi.nlm.nih.gov/entrez/eutils/elink.fcgi?dbfrom=pubmed&id=12414658&retmode=ref&cmd=prlinks%5Cnpapers3://publication/uuid/C1163A1A-24F2-45E5-BD68-595D11577D97>.
54. Wang W, Wyckoff JB, Goswami S, et al. Coordinated regulation of pathways for enhanced cell motility and chemotaxis is conserved in rat and mouse mammary tumors. *Cancer Res*. 2007;67(8):3505-3511. doi:10.1158/0008-5472.CAN-06-3714
55. Iwaya K, Oikawa K, Semba S, et al. Correlation between liver metastasis of the colocalization of actin-related protein 2 and 3 complex and WAVE2 in colorectal carcinoma. *Cancer Sci*. 2007;98(7):992-999. doi:10.1111/j.1349-7006.2007.00488.x
56. Yamaguchi H, Condeelis J. Regulation of the actin cytoskeleton in cancer cell migration and invasion. *Biochim Biophys Acta - Mol Cell Res*. 2007;1773(5):642-652. doi:10.1016/j.bbamcr.2006.07.001
57. Condeelis J, Segall JE. Intravital imaging of cell movement in tumours. *Nat Rev Cancer*. 2003;3(12):921-930. doi:10.1038/nrc1231
58. Yamaguchi H, Wyckoff J, Condeelis J. Cell migration in tumors. *Curr Opin Cell Biol*. 2005;17(5 SPEC. ISS.):559-564. doi:10.1016/j.ceb.2005.08.002
59. Frentzas S, Simoneau E, Bridgeman VL, et al. Vessel co-option mediates resistance to anti-angiogenic therapy in liver metastases. *Nat Med*. 2016;22(11):1294-1302. doi:10.1038/nm.4197
60. Pizarro-Cerdá J, Chorev DS, Geiger B, Cossart P. The Diverse Family of Arp2/3 Complexes. *Trends Cell Biol*. 2017;27(2):93-100. doi:10.1016/j.tcb.2016.08.001
61. Abella JVG, Galloni C, Pernier J, et al. Isoform diversity in the Arp2/3 complex determines actin filament dynamics. *Nat Cell Biol*. 2016;18(1):76-86. doi:10.1038/ncb3286
62. Kinoshita T, Nohata N, Watanabe-Takano H, et al. Actin-related protein 2/3 complex subunit 5 (ARPC5) contributes to cell migration and invasion and is directly regulated by tumor-suppressive microRNA-133a in head and neck squamous cell carcinoma. *Int J Oncol*. 2012;40(6):1770-1778. doi:10.3892/ijo.2012.1390
63. Moriya Y, Nohata N, Kinoshita T, et al. Tumor suppressive microRNA-133a regulates novel molecular networks in lung squamous cell carcinoma. *J Hum Genet*. 2012;57(1):38-45. doi:10.1038/jhg.2011.126

64. Hirsch HA, Iliopoulos D, Tsiachlis PN, Struhl K. Metformin selectively targets cancer stem cells, and acts together with chemotherapy to block tumor growth and prolong remission. 2010;69(19):7507-7511. doi:10.1158/0008-5472.CAN-09-2994.Metformin
65. Iliopoulos D, Hirsch H a, Struhl K. An epigenetic switch involving NF-κB, Lin28, let-7 microRNA, and IL6 links inflammation to cell transformation. *Biol Chem.* 2010;139(4):693-706. doi:10.1016/j.cell.2009.10.014.An
66. Elsberger B, Tan BA, Mitchell TJ, et al. Is expression or activation of Src kinase associated with cancer-specific survival in ER-, PR- and HER2-negative breast cancer patients? *Am J Pathol.* 2009;175(4):1389-1397. doi:10.2353/ajpath.2009.090273
67. Elsberger B, Fullerton R, Zino S, et al. Breast cancer patients clinical outcome measures are associated with Src kinase family member expression. *Br J Cancer.* 2010;103(6):899-909. doi:10.1038/sj.bjc.6605829
68. Brayford S, Bryce NS, Schevzov G, et al. Tropomyosin promotes lamellipodial persistence by collaborating with Arp2/3 at the leading edge. *Curr Biol.* 2016;26(10):1312-1318. doi:10.1016/j.cub.2016.03.028
69. Gunning PW, Schevzov G, Kee AJ, Hardeman EC. Tropomyosin isoforms: Divining rods for actin cytoskeleton function. *Trends Cell Biol.* 2005;15(6):333-341. doi:10.1016/j.tcb.2005.04.007
70. Lin JJC, Helfman DM, Hughes SH, Chou CS. Tropomyosin isoforms in chicken embryo fibroblasts: Purification, characterization, and changes in rous sarcoma virus-transformed cells. *J Cell Biol.* 1985;100(3):692-703. doi:10.1083/jcb.100.3.692
71. Schevzov G, Vrhovski B, Bryce NS, et al. Tissue-specific tropomyosin isoform composition. *J Histochem Cytochem.* 2005;53(5):557-570. doi:10.1369/jhc.4A6505.2005
72. Hannan AJ, Gunning P, Jeffrey PL, Weinberger RP. Structural compartments within neurons: Developmentally regulated organization of microfilament isoform mRNA and protein. *Mol Cell Neurosci.* 1998;11(5-6):289-304. doi:10.1006/mcne.1998.0693
73. Gunning P, O'Neill G, Hardeman E. Tropomyosin-based regulation of the actin cytoskeleton in time and space. *Physiol Rev.* 2008;88(1):1-35. doi:10.1152/physrev.00001.2007.
74. Warren KS, Lin JJC, McDermott JP, Lin JJC. Forced expression of chimeric human fibroblast tropomyosin mutants affects cytokinesis. *J Cell Biol.* 1995;129(3):697-708. doi:10.1083/jcb.129.3.697
75. Schevzov G, Whittaker SP, Fath T, Lin JJC, Gunning PW. Tropomyosin isoforms and reagents. *Bioarchitecture.* 2011;1(4):135-164. doi:10.4161/bioa.1.4.17897
76. Min K, Chae S, Kim D, et al. Fascin expression predicts an aggressive clinical course in patients with advanced breast cancer. *Oncol Lett.* 2015:121-130. doi:10.3892/ol.2015.3191
77. Mani S a, Guo W, Liao M, et al. The epithelial-mesenchymal transition generates cells with properties of stem cells. *Cell.* 2009;133(4):704-715. doi:10.1016/j.cell.2008.03.027.
78. Polyak K, Weinberg RA. Transitions between epithelial and mesenchymal states: Acquisition of malignant and stem cell traits. *Nat Rev Cancer.* 2009;9(4):265-273. doi:10.1038/nrc2620
79. Ahna R. Skop1, 2, *, †, Hongbin Liu3, John Yates III3, Barbara J. Meyer1, 2 and RH. Dissection of the Mammalian Midbody Proteome Reveals Conserved Cytokinesis Mechanisms. 2004. doi:10.1126/science.1097931.Dissection
80. Hu C-K, Coughlin M, Mitchison TJ. Midbody assembly and its regulation during cytokinesis. *Mol Biol Cell.* 2012;23(6):1024-1034. doi:10.1091/mbc.E11-08-0721
81. Greenbaum MP, Iwamori T, Buchold GM, Matzuk MM. Germ cell intercellular bridges. *Cold Spring Harb Perspect Biol.* 2011;3(8):1-18. doi:10.1101/cshperspect.a005850
82. Austefjord MW, Gerdes HH, Wang X. Tunneling nanotubes: Diversity in morphology and structure. *Commun Integr Biol.* 2014;7(2):1-5. doi:10.4161/cib.27934
83. González-Méndez L, Seijo-Barandiarán I, Guerrero I. Cytoneme-mediated cell-cell contacts for hedgehog reception. *Elife.* 2017;6:1-24. doi:10.7554/eLife.24045
84. Krummel MF, Cahalan MD. The immunological synapse: A dynamic platform for local signaling. *J Clin Immunol.* 2010;30(3):364-372. doi:10.1007/s10875-010-9393-6
85. Piragyte I, Jun C-D. Actin engine in immunological synapse. *Immune Netw.* 2012;12(3):71-83. doi:10.4110/in.2012.12.3.71
86. Bunnell SC, Hong DI, Kardon JR, et al. T cell receptor ligation induces the formation of dynamically regulated signaling assemblies. *J Cell Biol.* 2002;158(7):1263-1275. doi:10.1083/jcb.200203043